Review

Recent Advances on Metal Oxide Based Nano-Photocatalysts as Potential Antibacterial and Antiviral Agents

Jai Prakash [1,2,*], Suresh Babu Naidu Krishna [3], Promod Kumar [2], Vinod Kumar [4], Kalyan S. Ghosh [1], Hendrik C. Swart [2], Stefano Bellucci [5] and Junghyun Cho [6]

[1] Department of Chemistry, National Institute of Technology Hamirpur, Hamirpur 177005, Himachal Pradesh, India
[2] Department of Physics, University of the Free State, Bloemfontein 9300, South Africa
[3] Department of Biomedical and Clinical Technology, Durban University of Technology, Durban 4000, South Africa
[4] Department of Physics, College of Natural and Computational Science, Dambi Dollo University, Dambi Dollo P.O. Box 260, Ethiopia
[5] INFN Laboratori Nazionali di Frascati, Via Enrico Fermi 40, 00044 Frascati, Italy
[6] Department of Mechanical Engineering & Materials Science and Engineering Program, State University of New York (SUNY), Binghamton, NY 13902-6000, USA
* Correspondence: jaip@nith.ac.in

Abstract: Photocatalysis, a unique process that occurs in the presence of light radiation, can potentially be utilized to control environmental pollution, and improve the health of society. Photocatalytic removal, or disinfection, of chemical and biological species has been known for decades; however, its extension to indoor environments in public places has always been challenging. Many efforts have been made in this direction in the last two–three years since the COVID-19 pandemic started. Furthermore, the development of efficient photocatalytic nanomaterials through modifications to improve their photoactivity under ambient conditions for fighting with such a pandemic situation is a high research priority. In recent years, several metal oxides-based nano-photocatalysts have been designed to work efficiently in outdoor and indoor environments for the photocatalytic disinfection of biological species. The present review briefly discusses the advances made in the last two to three years for photocatalytic viral and bacterial disinfections. Moreover, emphasis has been given to the tailoring of such nano-photocatalysts in disinfecting surfaces, air, and water to stop viral/bacterial infection in the indoor environment. The role of such nano-photocatalysts in the photocatalytic disinfection of COVID-19 has also been highlighted with their future applicability in controlling such pandemics.

Keywords: antibacterial; antiviral; air/water disinfection; surface decontamination; metal oxide semiconductors; nano-photocatalysts

1. Introduction

Even with the fast growing technology and industrial developments, the modern world is still lacking in the control of environmental and health issues. The best example is the current COVID-19 pandemic, which has made us realize that the modern world should also take care of the development of novel technologies, materials and medical innovations to control such health- and environment-related issues [1]. Various unwanted components present in the environment affect human health directly or indirectly. In this context in particular, different microbial pathogens such as viruses, bacteria, protozoa, etc. present in the environment may sometimes threaten human health and cause dangerous infectious illnesses [1,2]. Recent developments suggest that nanotechnology-based methods and materials could be alternate options with the huge potential for controlling such bacterial/viral outbreaks [3–6] which have been a serious issue and increased at a disquieting rate over the past decades [2].

Photocatalysis, which uses nano-photocatalysts, is one of the unique processes occurs in the presence of solar radiation [7,8]. This process is promising for the control of environmental issues and for improving the health of the society due to the presence of unspent solar energy on the Earth [9,10]. Photocatalysis has multifunctional applications in the field of environmental studies, including the photocatalytic degradation of toxic/harmful organic compounds and gases [11–13], and the photocatalytic viral and bacterial disinfection of water, air, or on surfaces, which ultimately protects the environment and improves human health [14–17]. Photocatalytic removal or disinfection of such species is a promising and environmentally friendly process using suitable photocatalysts under the influence of solar radiation. Furthermore, it is also very cost-effective and promising in the open environment [1,9]. In recent years, several metal oxide semiconductor photocatalysts such as TiO_2, ZnO, CuO, WO_3, etc. have been designed as visible active photocatalysts. Their properties have been improved through some modifications which enable them to work efficiently in solar light towards photocatalytic degradation and disinfection of chemical and biological species [18,19], respectively. These are found to be very useful for disinfecting surfaces, air, and water by killing several microorganisms i.e., bacteria and fungi, and inactivating several viruses including influenza virus, hepatitis C virus, coronavirus, etc., [20]. These photocatalysts exhibit oxidative capabilities via the photocatalytic production of cytotoxic reactive oxygen species (ROS) as shown in Figure 1 for photo-degradation/inactivation of such species in outdoor as well as indoor environment. It has been found to be very beneficial for the treatment of various bacterial/viral diseases such as measles, influenza, herpes, Ebola, current COVID-19, etc., [1,2] as is shown schematically in Figure 2.
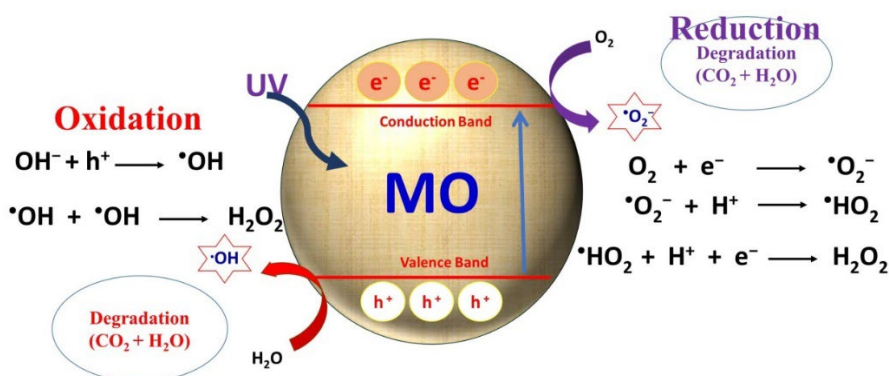
Figure 1. Photocatalytic mechanism of metal oxide nano-photocatalysts towards photocatalytic degradation of chemical species [12].

These semiconductor nano-photocatalysts are potential candidates as next-generation antibiotics and antiviral agents to deal with multi-drug-resistant pathogens and viruses, respectively, owing to their outstanding antibacterial/viral performance. The action of photocatalytic inactivation/degradation of these nano-photocatalysts on various bacterial and viruses has been successfully explained by several authors; however, the proposed mechanisms are still under debate and continuous investigations are going on by the scientific community [11,21–23]. This review covers briefly recent advances carried out in this field using metal oxide nano-photocatalysts with an emphasis on the understanding of photomechanism processes and potential applications in the environment. The role of such nano-photocatalysts in photocatalytic disinfection of COVID-19 has also been highlighted, along with their future applicability in controlling such pandemic situations.

Figure 2. Schematic representation of photodegradation of viruses/microbes in outdoor as well as indoor environment using metal oxide nano-photocatalysts [1].

2. Metal Oxide Based Nano-Photocatalysts: Antibacterial and Antiviral Mechanisms

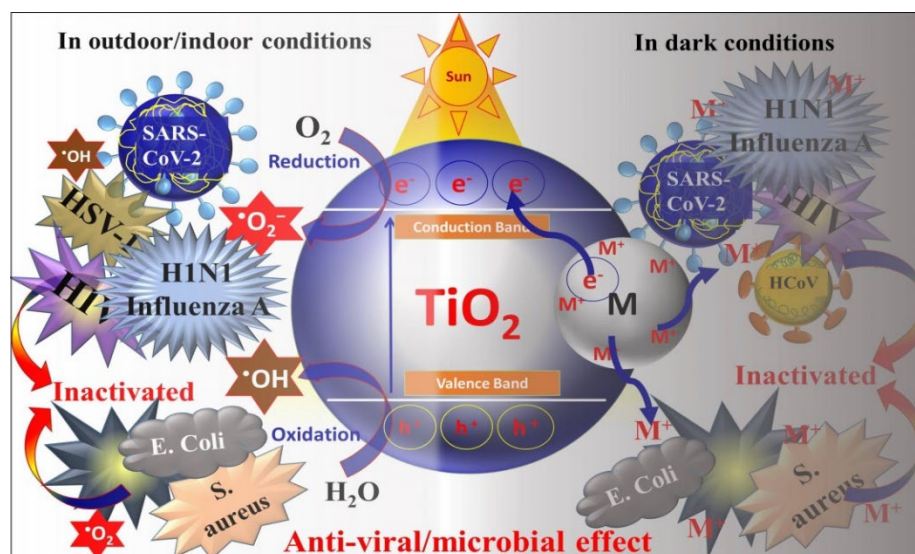The photocatalysis method of disinfection using metal oxide semiconductors shows great potential in outdoor and indoor environments as compared to the conventional methods for the removal of bacteria or viruses. These nano-photocatalysts can effectively inactivate the bacteria and viruses in the presence of light radiation under ambient conditions without producing any other by-products as compared to that of using chemicals [1,24].

Metal oxide semiconductor-based nano-photocatalysts such as TiO_2, and ZnO have been extensively investigated for inactivation of several bacteria and viruses. The basic mechanism behind their photoinduced inactivation involves the photocatalytic production of short-lived but effective biocidal ROS, i.e., hydroxyl radicals ($\bullet OH$), superoxide ($\bullet O_2^-$), and hydrogen peroxide (H_2O_2), through photochemical redox reactions under light irradiation. [25,26]. The formation mechanism of various ROS in various cases is shown in Figure 3. Such an effectively biocidal ROS further inactivates the bacteria and viruses by damaging deoxyribonucleic acid (DNA), Ribonucleic acid (RNA), proteins, and lipids [2,17,26,27]. The generation of ROS and the disinfection of bacteria and virus, including severe acute respiratory syndrome coronavirus 2 (SARS-CoV-2) virus inactivation, are shown schematically in Figure 3a–c.

Under the influence of ultra-violet (UV) light radiation, these nano-photocatalysts absorb the radiation resulting in excitation and promotion of valance band (VB) electrons into the conduction band (CB). The holes in VB interact with the adsorbed water molecules and produce active OH and H_2O_2 free radicals. These free radicals are powerful oxidants which generally oxidize the components/chemical in the shell and capsid of the bacteria and viruses [27]. Subsequently, whereas electrons in CB generally reduce the atmospheric O_2 (or available from the medium) and produce $\bullet O_2^-$ radicals [27,28]. Similarly, $\bullet O_2^-$ radicals produced in photocatalysis are effective in rupturing the capsid shell that results in the leakage and rapid destruction of capsid proteins and RNA [29] (Figure 3b,c).
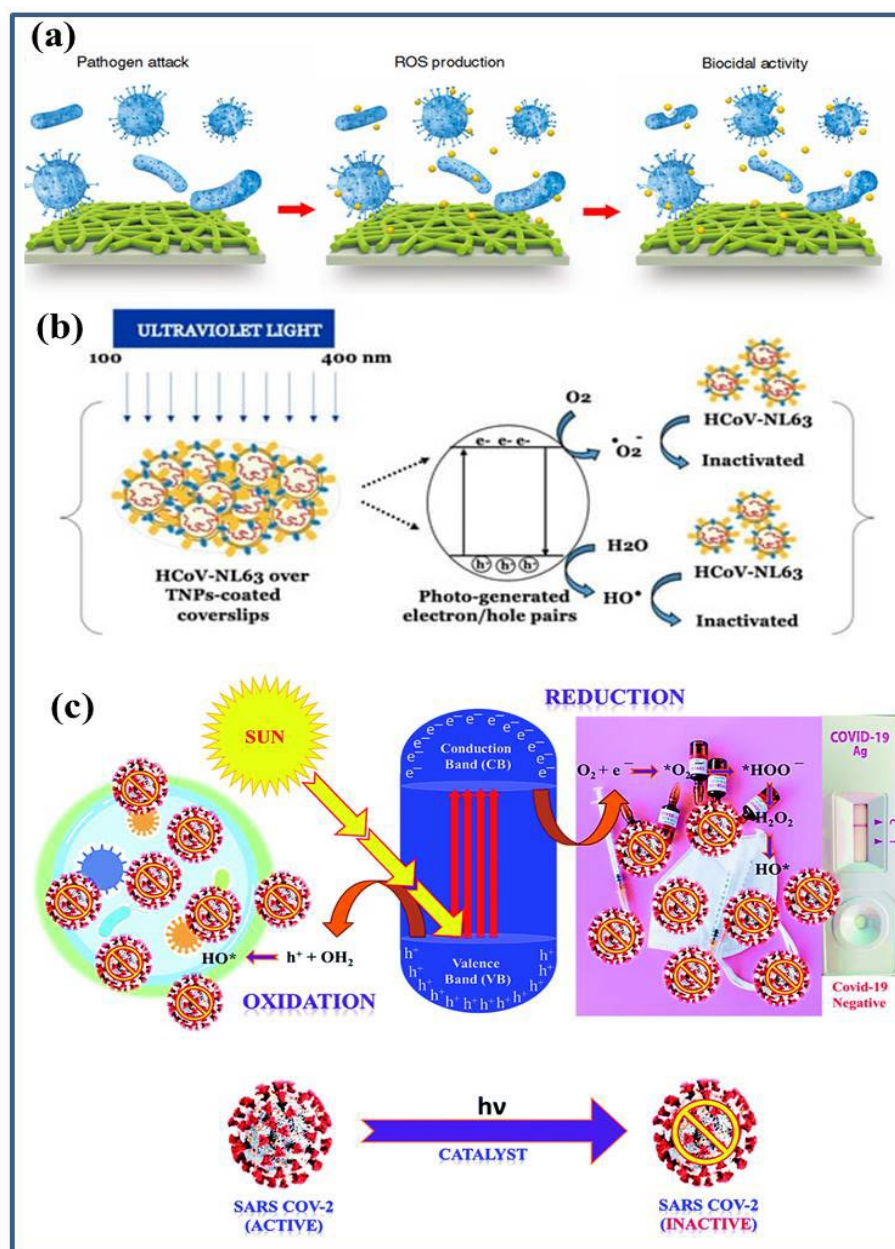
Figure 3. Schematic representation of photocatalytic disinfection of: (**a**) bacteria [26]; (**b**) HCoV-NL63 virus [28]; and (**c**) SARS-CoV-2 virus [27]. Under the influence of light irradiation, the photocatalysts produce electrons and holes that undergo oxidation and reduction processes with O_2 and H_2O generating strong free radical on their surfaces. These radicals interact with the adsorbed bacteria or viruses and inactivate them.

The ROS as produced generally attack or interact with the cytoplasmic membrane and cell wall of the bacteria or viruses during the inactivation mechanism [30]. However, the rate of photo inactivation/disinfection depends on the photocatalyst used and the amount of ROS produced under the influence of the available wavelength of light irradiation, and also depends on the internal as well as external cell structures of the type of pathogens, because all the bacteria or viruses do not have similar cell wall and membrane structures. These components may have complicated layered structures and contain various types of RNA/DNA, proteins, or enzymes [1,27,30]. For instance, cyclobutene pyrimidine dimers (CPDs) and pyrimidine-6,4-pyrimidone (6.4 PP) photoproducts, together with the Dewar-valence isomers, are the most studied and best described UV-induced photoreactions between and within nucleic acids [30,31]. Following UV light exposure, pyrimidine dimers

(see Scheme 1) are formed. CPD and 6,4PP dimers are mainly responsible for bending the double helix 7–9 and 44 degrees, respectively, once they are formed. DNA replication is stopped because of these alterations.
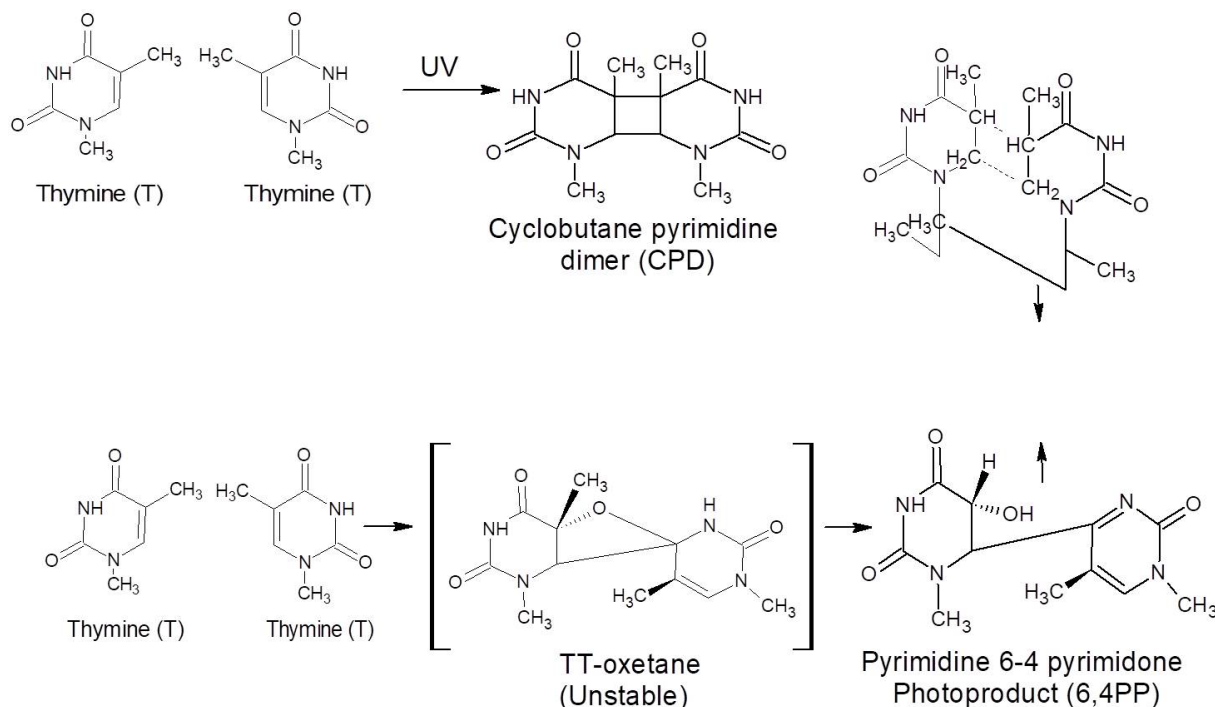
Scheme 1. Schematic diagram of how pyrimidine dimers form after DNA is exposed to UV light. between two adjacent thymine (T) nitrogenous bases, the production of cyclobutane pyrimidine dimers (CPDs); and pyrimidine-6.4-pyrimidone photoproducts (6.4 PP). Similar reactions for uracil in the case of RNA could take place (U) [30].

Because of their wide band gap, the TiO_2 (3.2 eV) and ZnO (3.37 eV) nano-photocatalysts absorb the high energy UV radiation. This limits their potential photocatalytic applicability more efficiently in outdoor environments under the sunlight because it has only 3–5% UV radiation. Furthermore, photocatalytic disinfection processes in indoor environments are challenging, and modifications of these metal oxide nano-photocatalysts to make them visible light active photocatalysts need to be explored [9,25]. There are several ways to modify these nano-photocatalysts, such as doping with metals/non-metals [32], surface modification via sensitizing or heterojunction formation [10,33] with other functional nanomaterials such as noble metals, carbon based nanomaterials (i.e., graphene, carbon nanotubes, graphene oxide, etc.) [8,34] other metal oxides, etc. [35–37] Emphasis has been given to enhance the surface area, prevent the recombination of photogenerated charge carriers, and bandgap modification to extend into visible light absorption for effective use in ambient conditions [11,38]. For example, Yu et al. [39,40] demonstrated the enhanced photocatalytic activity of mesoporous TiO_2 via F doping attributed to the stronger absorption in UV-visible region with a red shift in the band gap transition. Fe doped TiO_2 were found to be very effective in visible region with excellent antifungal activities under natural environment [41]. Similarly, Ag doped ZnO [23] and TiO_2 NPs [11] showed better antibacterial activities in normal room conditions due to Ag ion-induced visible light activity in these nano-photocatalysts. These nano-photocatalysts, modified with plasmonic noble metals [42–44], are effective antibacterial and antiviral agents in dark conditions [1,45]. Interestingly, such nano-photocatalysts have also been used as memory catalysis because of their unique talent to retain the catalytic performance in dark conditions [33,45,46]. For example, Tatsuma et al. [47] demonstrated that TiO_2–WO_3 heterojuction nanocomposite photocatalyst films could be charged by UV light irradiation

which showed good antibacterial effect on Escherichia coli in dark environment. Similarly, Ag-modified TiO_2 films were also shown to exhibit disinfection memory activity [45].

As discussed above, a great deal of research has been performed in real practical applications of such nano-photocatalysts. Recent developments show that modified metal oxide nano-photocatalysts are promising disinfection agents in indoor environments in ambient room conditions when applied in the form of surface coating/thin films on commonly used surfaces in hospitals, offices, home, etc. Additionally, potential practical applications have been carried out which show excellent results while using these nanomaterials for the disinfection of polluted water and air (in indoor as well as outdoor environments) which show their potential to combat pandemics such as COVID-19. The disinfection applications of such nano-photocatalysts in air, water and on surfaces have been discussed in the next sections, with an emphasis on their mechanism of actions.

3. Recent Advances on Metal Oxide Based Nano-Photocatalysts as Potential Antibacterial and Antiviral Agents

3.1. TiO₂ Based Nano-Photocatalysts as Potential Antibacterial and Antiviral Agents

The sudden pandemic spread due to the novel SARS-CoV-2 virus has made the world realize that the development of simple and cost-effective nanomaterials-based technology is needed. Meanwhile, a great deal of research has been focused on developing various types of nanomaterials to fight against disease-causing bacteria and viruses which could be effective in water, air and on surfaces [30]. More emphasis has been given to developing promising materials to be used in indoor spaces such as hospitals, homes, and other public places to minimize the health- and environment-related risks [1]. As discussed in the previous section, metal oxide-based nano-photocatalysts are promising mainly in outdoor circumstances due to their light absorption activity cum disinfection ability. However, these nanomaterials have been modified to function in many ways [48–53], and have been explored in the case of indoor disinfection activities, including surface decontamination. TiO_2 is one of the most used and studied metal oxide semiconductor nano-photocatalysts for disinfection caused by bacteria and viruses in the last decades. UV and visible light activation techniques have been used as promising approaches for the outdoor and indoor disinfection applications of TiO_2. TiO_2 has been researched for last many decades owing to its promising photocatalytic activity. The sole TiO_2 is known to be an active photocatalyst under UV light radiation and transparent to visible light due to its bandgap of 3.2 eV [32,54,55]. It is a fascinating material because of its tunable characteristics and the existence of its different forms. Several efforts have been made to enhance its photocatalytic activity towards removal or disinfection under visible light, which is still challenging under ambient conditions [56–61].

Krumdieck et al. [56] developed a TiO_2 based nanocomposite coating for stainless steel-made surfaces such as door handles, bed rails and other high touch surfaces which could be the main source of spreading germs/infections in hospitals. The coating was made of nanostructured anatase, rutile dendrites and carbon (NsARC), with promising structural and adhesive properties (Figure 4a). The NsARC coating showed excellent antibacterial activity under sunlight along with a significant disinfection effect in dark conditions (Figure 4b). The enhanced photocatalytic activity (greater than 3-log reduction in viable *E coli*) was attributed to the rutile-anatase heterojunctions, nanostructured single crystals with high surface area and the low migration path length of the charge carriers (Figure 4c).
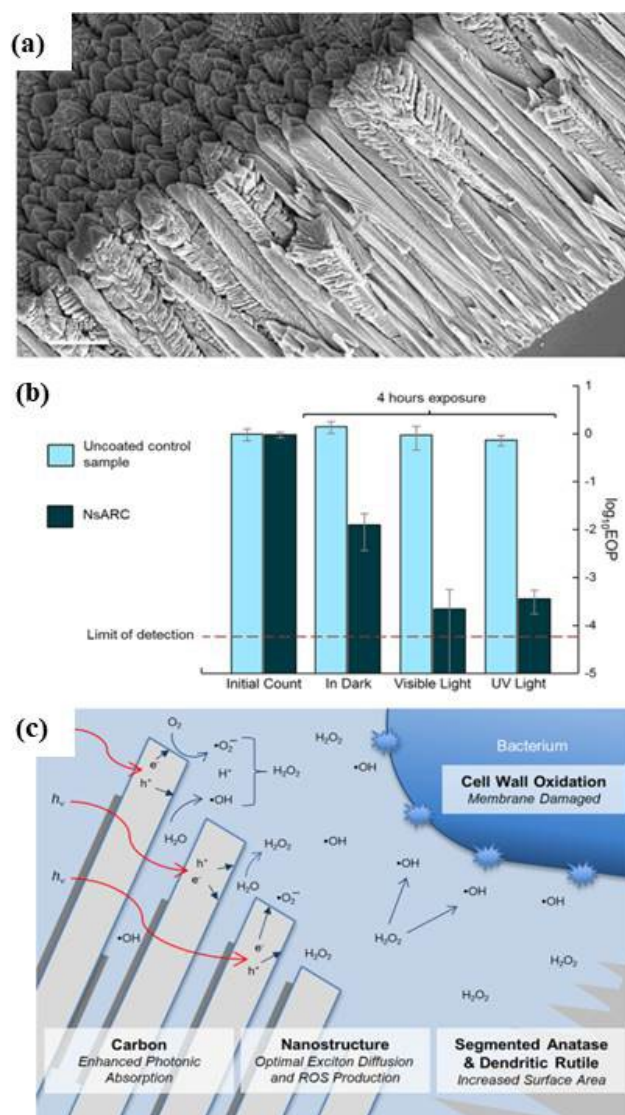
Figure 4. (**a**) Secondary electron microscopy (SEM) image of NsARC nanocomposite; (**b**) antibacterial performance of NsARC coated stainless steel on E. coli in different conditions including in dark conditions also; and (**c**) mechanisms of disinfection of antibacterial activity of NsARC on *E.coli* [56].

Reduced graphene oxide (rGO) modified TiO_2 composite photocatalysts under artificial solar light showed enhanced antibacterial performance as compared to only TiO_2 against *E. coli* that was attributed to a change on the surface properties due to rGO. Figure 5a shows the SEM micrograph of *E. coli* bacterial cell and Figure 5b shows the *E. coli* covered with rGO-TiO_2 nanocomposites. After sunlight exposure, bacterial cells were damaged as shown in Figure 5c,d [57]. Similarly, Zhou et al. [58] reported the excellent antibacterial behavior of rGO-TiO_2 nanocomposites under UV and visible light environment against *E. hormaechei*. Dhanasekar et al. [60] reported on rGO-Cu doped TiO_2 nanocomposites that showed excellent ambient light antibacterial performance against several bacteria (Figure 5e). The material modification i.e., doping [62,63] and forming the composite with rGO, enhanced the visible light activity in ambient conditions by reducing the recombination of photogenerated charge carriers and their transport, respectively, for powerful ROS production for activation. From a practical application point of view, the nanocomposite was explored as a coating embedded in a polymer film/coating [37,64] which exhibited equal performance, showing the potential for its use as an antibacterial coating for different applications in surface protection. Similarly, complete disinfection under low intensity-simulated solar light irradiation was shown by Bonnefond et al. [61] using hybrid

acrylic/TiO$_2$ films. This kind of photocatalytic film with a self-cleaning ability [54] and high disinfection performance could be applied for surfaces in ambient conditions in the indoor environment to stop the spreading of bacterial germs/viruses, etc. (Figure 5f).
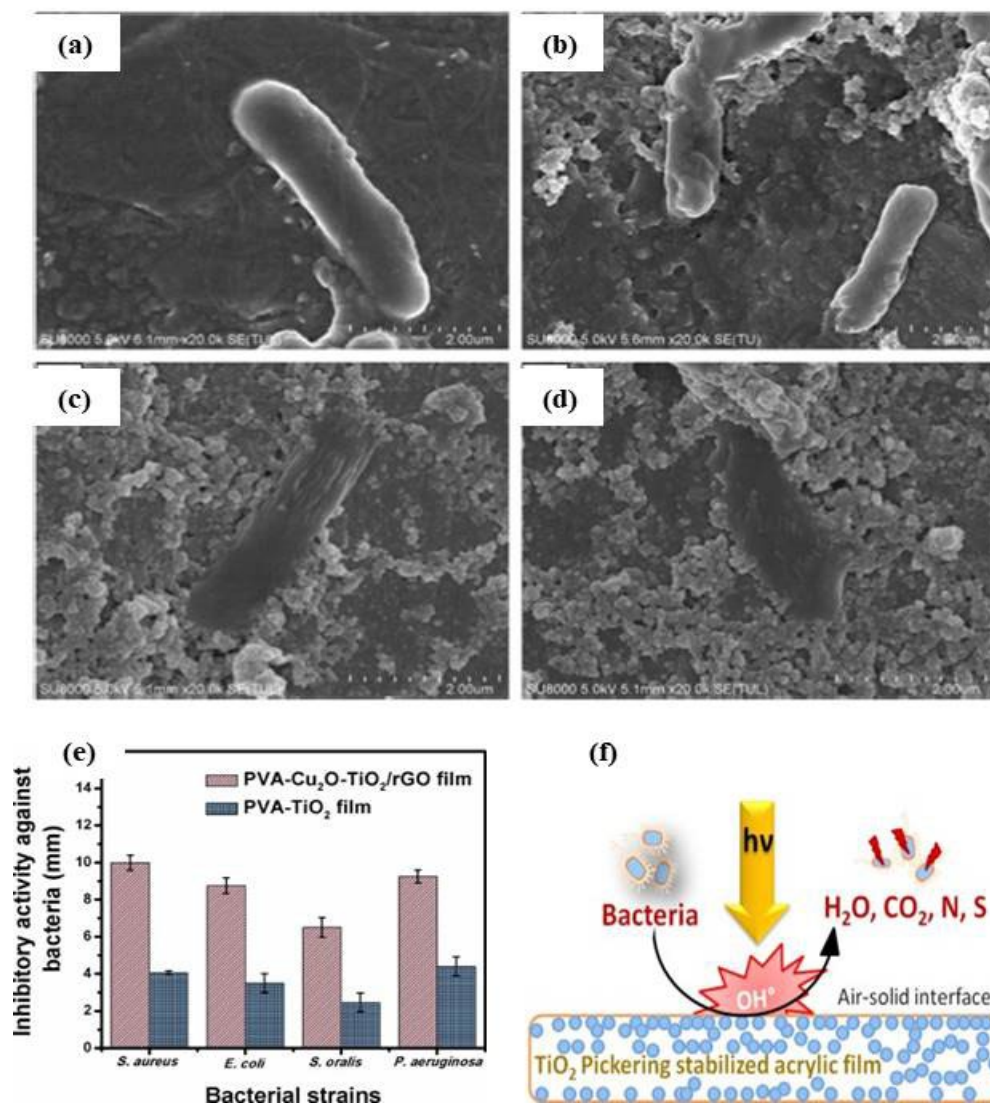
Figure 5. SEM images of (**a**) *E. coli* bacterial cell; (**b**) *E.coli* covered with TiO$_2$-rGO before sunlight irradiation; (**c**,**d**) damaged bacterial cells after sunlight irradiation (reproduced with permission from Ref. [57] Copyright 2018-Elsevier); (**e**) antibacterial effect of rGO-Cu doped TiO$_2$ nanocomposites in ambient light against several microbes (reproduced with permission from Ref. [60] Copyright 2018-Elsevier) and (**f**) self-cleaning ability hybrid acrylic/TiO$_2$ films (reproduced with permission from Ref. [61]. Copyright 2015-Elsevier).

The usse of photocatalysts in airborne bacterial disinfection is very important in indoor environment but very challenging [65–67]. Hernández-Gordillo et al. [65] demonstrated that CuO- and CdS-modified TiO$_2$ monoliths surfaces could be efficient for the removal and inactivation of airborne bacteria under visible light irradiation in a continuous flow photoreactor. The flow cytometry and SEM micrograph results were used to study the damaging of the bacteria. The SEM micrographs exhibited the collapsing of the cell membrane of bacteria due to the lipid peroxidation because of interaction with ROS generated on the monolith surface as shown in Figure 6a–g. The photocatalytic inactivation of TiO$_2$/CdS monoliths, was found to be maximum (99.9%). Similarly, Valdez-Castillo et al. [68] demonstrated bioaerosols disinfection using perlite-supported ZnO and TiO$_2$. It was found that

these photocatalysts showed better disinfection performance leading to cell death. It was concluded that these photocatalytic systems could be potentially used for practical applications in removing viable airborne microorganisms from air.

Various TiO_2 based floating photocatalysts were proposed to efficiently disinfect the polluted water [69,70]. Varnagiris et al. [69] reported on the disinfection application of C-doped TiO_2 films supported on high-density polyethylene (HDPE) beads in polluted water as floating photocatalysts. Interesting results of microbial disinfection i.e., 95% of *Salmonella typhimurium* bacteria in water environment along with recyclability of the substrates were observed. Similarly, they used polystyrene (PS) beads to coat with photocatalytic TiO_2 and used for the photocatalytic disinfection of *E. coli* in antibacterial contaminated water as shown in Figure 6h [70]. More than 90% of inactivation was observed. Recently, Sboui et al. [71] proposed TiO_2 and Ag_2O nanocomposites immobilized on cellulose paper as an excellent floating photocatalytic antibacterial system against *E. coli*.
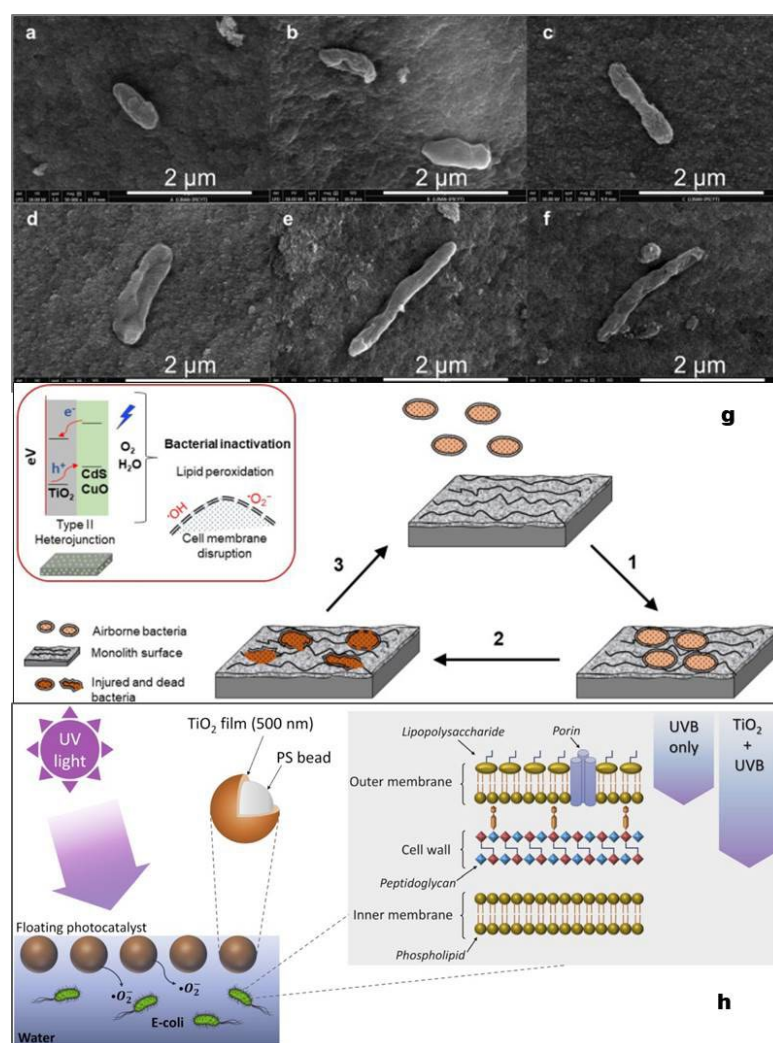
Figure 6. SEM images of bioaerosols adsorbed on TiO_2 based monoliths: (**a**,**b**) m-TiO_2/CdS; (**c**,**d**) m-TiO_2/CuO and (**e**,**f**) m-TiO_2, before and after photocatalysis, respectively; (**g**) Bioaerosol inactivation mechanism in the continuous flow photoreactor. (1) airborne bacteria are adsorbed on the monoliths. (2) photocatalysis produces ROS affecting the adsorbed bacteria. (3) inactive bioaerosols are released, the monolith surface becomes available to adsorb new airborne bacteria. Inset shows schematically the generation of reactive oxygen species from the monolith surface under blue light, causing lipid peroxidation (reproduced with permission from Ref. [65] Copyright 2021-Springer Nature); (**h**) schematic of *E. coli* bacteria hoto-decomposition using floating photocatalyst (reproduced with permission from Ref. [70]. Copyright 2020-Elsevier).

Tong et al. [29] demonstrated that TiO$_2$ coating could be efficiently used to inhibit *hepatitis C virus* (HCV) infection under the effect of weak indoor light. It was explained that OH radicals (as compared to ●O$_2^-$ radicals) produced by photo-activated TiO$_2$ were mainly responsible for damaging RNA genome by inactivating the virus without destroying the virion global structure and contents. The overall experiment has been described in Figure 7a. More details can be found elsewhere [29]. Figure 7b shows the effect of photoactivated TiO$_2$ on the inhibition of HCV infection in different conditions (light/off). Figure 7c,d show that there is no change in the quantity of HCV protein and RNA in the virions which proves that there is no destruction by photoactivated TiO$_2$-produced ROS on the virion structures. Figure 7e,f show the effect of photocatalytic treatment on the cells post-transfection. It signified that there were no viral amplifications after the photocatalytic TiO$_2$ inactivation suggesting that although there was no change in the amount of viral RNA after interaction with photocatalytic TiO$_2$ but their biological activity was impaired. This resulted in the realization of the damaging effect of RNA genome for the inactivation without destroying the virion structure. The formation of ROS was studied by electron spin-resonance (ESR) spectroscopy measurements as shown in Figure 7g,h. The ESR results exhibited presence of both ●OH and ●O$_2^-$ radicals under the effect of light in indoor environments, whereas no peaks corresponding to these radicals were observed in dark conditions [29]. These results show that ROS were produced and played a major role in the inactivation of the HCV viruses.
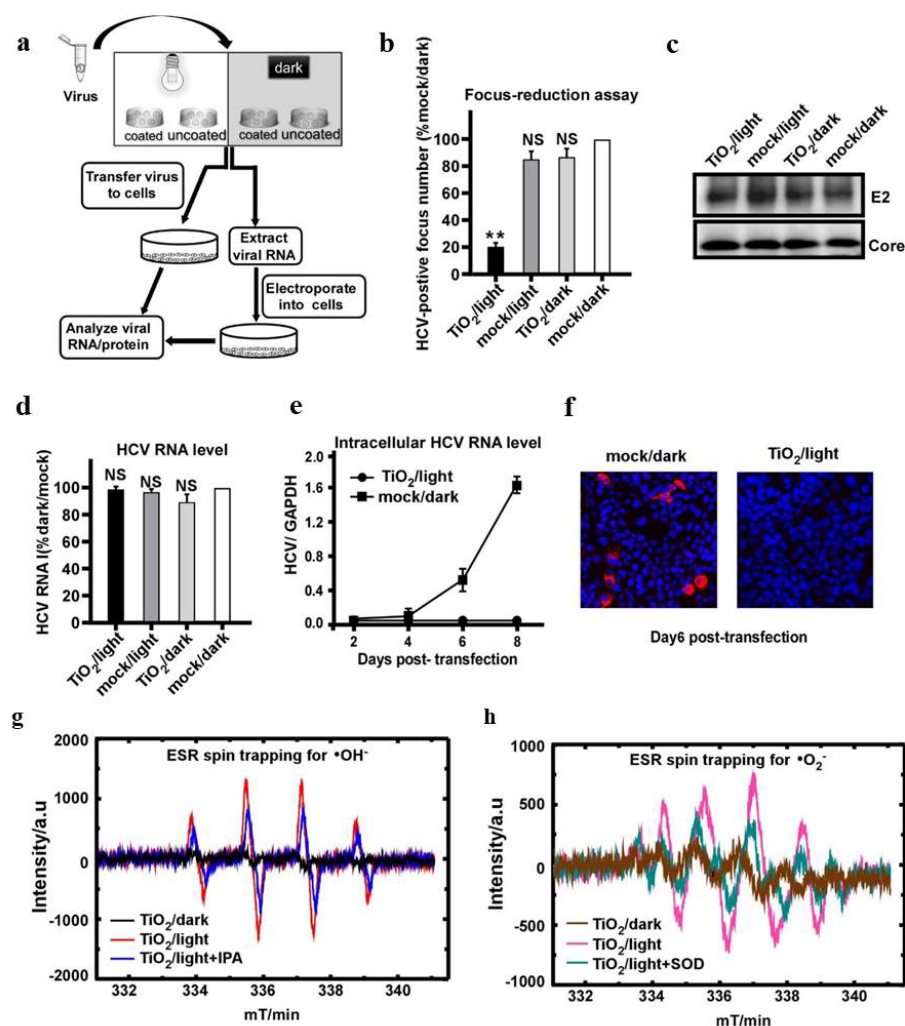

Figure 7. (**a**) Schematic representation of TiO$_2$ photocatalytic inhibition of HCV infection in dark and light; (**b**) the HCV-positive foci as determined by immunofluorescence of HCV NS3 proteins and

expressed as the percentage of the mock/dark group; (**c,d**) HCV E2 and Core proteins (**c**) and genome RNA (**d**) in the input virions after the TiO2/light treatment (as quantified by Western blotting and RT-qPCR, respectively); (**e**) the intracellular HCV RNA levels; (**f**) immunofluorescence of NS3 proteins (red) transfected with the extracted RNA from TiO_2/light treated virions on day six post-transfection. Nuclei (blue) were stained with Hoechst dye; (**g,h**) ESR results show the presence of both •OH and •O_2− radicals under the effect of light in indoor environment whereas, no peaks corresponding to these radicals were observed in the dark conditions (reproduced with permission from Ref. [29] Copyright 2021-Elsevier).

Similarly, Khaiboullina et al. [28] studied the photocatalytic TiO_2 coating effect on HCoV-NL63 virus, which is known to be an alpha coronavirus causing acute respiratory distress symptoms. It was found that TiO_2 coating effectively inactivated HCoV-NL63 viruses by reducing the viral genomic RNA stability and virus infectivity. The HCoV-NL63 viruses, placed on TiO_2 nanoparticles (NPs) coated surfaces, were treated with UV, and complete disinfection was observed even after one minute of UV light exposure. In order to make sure of the disinfection activity, a virus infectivity assay was carried out by adding the recovered viruses (from TiO_2 coated and uncoated surfaces after UV light exposure) onto the monolayer of HEK293L cells. As observed in immunofluorescent signals from HEK293L cells as shown in Figure 8 (when compared A–D to E–H), it was found that those HCoV-NL63 viruses taken from TiO_2 coated surfaces after UV exposure were completely inactivated, while those on uncoated TiO_2 surface were not fully inactivated and live infectious viruses were detected. The overall experiment concluded that the viruses on the TiO_2 coated surface could be disinfected very quickly as compared to that of the uncoated surface under the UV light exposure [28].
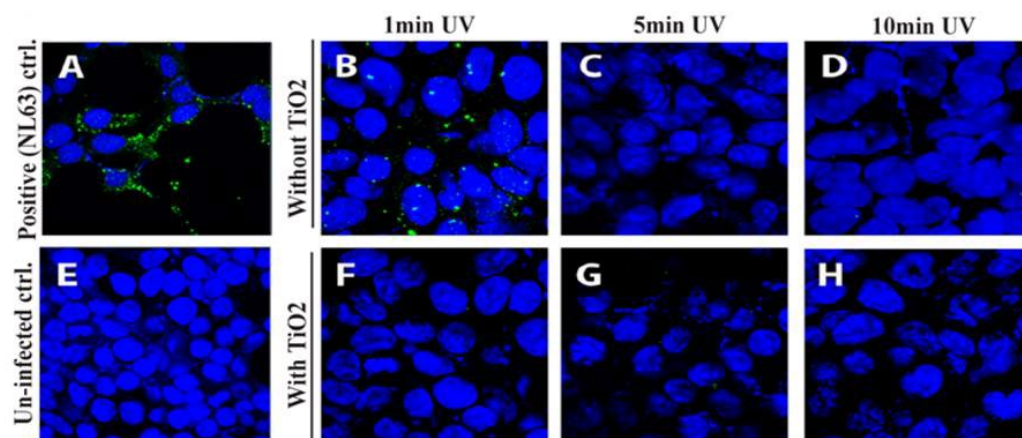
Figure 8. Post-UV treatment, HCoV-NL63 virus was collected and subjected to the infection of HEK293L monolayer. Viral protein, indicator of virus infectivity and replication, was detected by immune localization through IFA (green fluorescent dots): (**A**) NL63 infection (positive control); (**B**) 1 min UV light exposure without TiO_2; (**C**) 5 min UV light exposure without TiO_2; (**D**) 10 min UV light exposure without TiO_2; (**E**) uninfected control (negative control); (**F**) 1 min UV light exposure with TiO_2; (**G**) 5 min UV light exposure with TiO_2; and (**H**) 10 min UV light exposure with TiO_2 [28].

Mathur et al. [72] demonstrated that the UV activation killing mechanism of TiO_2 could be effectively used for purifying the air in a closed cabin by killing living organic germs, bacteria, pathogen viruses, etc., from the cabin air in recirculation mode. It was suggested that by using this model, various air condition systems could be designed to make the cabin free of bacterial and viral infections. Similarly, Matsuura et al. [20] studied the disinfection of SARS-CoV-2 in liquid/aerosols using coated TiO_2 nano-photocatalyst activated by a light-emitting diode in an air cleaner. The photocatalytic disinfection was explained by observing the virion morphology using transmission electron microscopy (TEM) by detecting damaged viral RNA and proteins as shown in Figure 9a. These

nano-photocatalysts are shown to be very promising antiviral coatings for protecting surfaces against the spread of viruses such as COVID-19 [73–75]. Recently Uppal et al. [74] performed the study of a TiO_2 photocatalytic coating for virucidal activity against the HCoV-OC43 virus which is a member of the beta coronaviruses family just like SARS-CoV-2 under the influence of UV irradiation using T-qPCR and virus infectivity assays. It was found that the glass surface coated with TiO_2 exhibited better antiviral response as compared to uncoated glass against the virus. UV exposure reduced the viral RNA copies and the infectious virus with increasing exposure time and a 60 min exposure completely disinfected the viruses, as shown in Figure 9b,c.
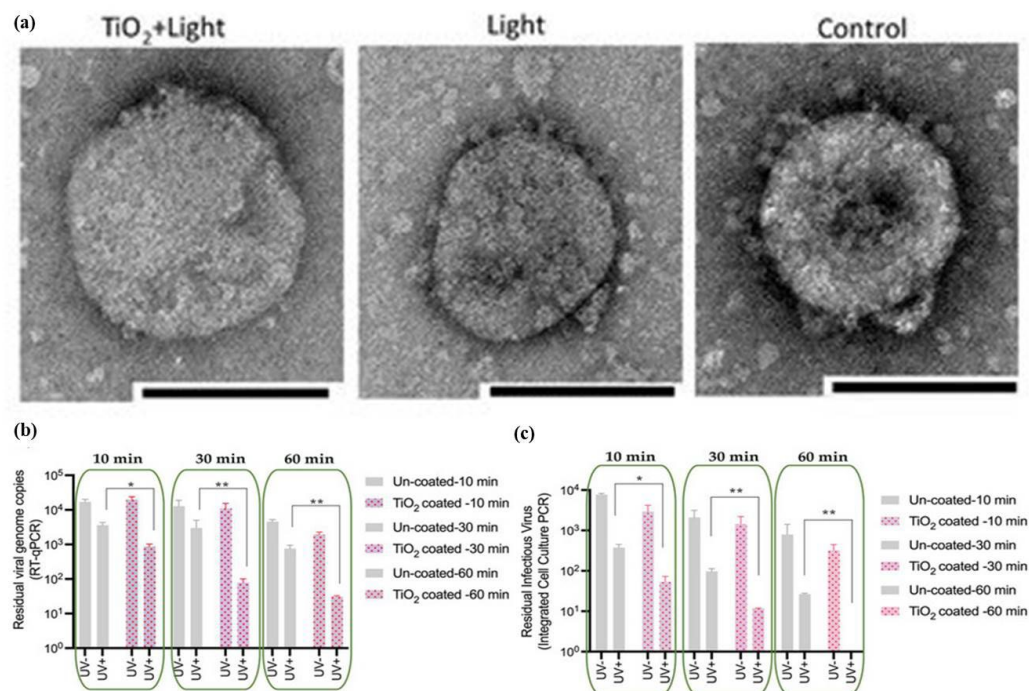

Figure 9. (**a**) TEM images SARS-CoV-2 virus showing the effect of TiO_2 and UV irradiation on the stability of human coronavirus [20]; TiO_2 photocatalytic coating for virucidal activity against the HCoV-OC43 virus (**b**) followed by exposure to UVA light (Post UV-irradiation, total viral RNA was extracted for the detection of intact viral genome copies via RT-qPCR.) (**c**) followed by infection of A549-hACE2 cells (total viral RNA was extracted to detect intracellular viral genome copies following infection and replication) [74].

Only UV exposure has also been reported to be effective against corona and other viruses spreading but has limited applications in surgical instruments, respiratory masks, and indoor environments that are also very challenging [76]. TiO_2 coating on the tile surface was also studied to investigate the effect of the coating against virus contamination keeping in mind public places such as hospitals. It was found that ambient light could not have any effect on the viral viability but when the tiles were coated with TiO_2/Ag–TiO_2, complete inactivation of the viruses under the same ambient light conditions in 5 h was exhibited. The coating was also found very stable after 4 months and showed similar disinfection response in indoor environment [77]. Nakano et al. [73] reported on antiviral effect of Cu_xO/TiO_2 induced inactivation of SARS-CoV-2 virus, including its Delta variant [78] under dark conditions as well as light irradiation using a normal white fluorescent bulb. Figure 10a,b show the morphology of the nanocomposites of Cu_xO/TiO_2 photocatalyst and the enhanced visible light absorption spectra respectively. Role of $CuxO$/TiO_2 photocatalyst was examined against SARS-CoV-2 virus which revealed the inactivation through damaging proteins and RNAs in the virus even under the dark conditioned. The damaging action was enhanced further under the white bulb illumination in presence of visible light active

Cu_xO/TiO_2 photocatalyst as shown in the graph of Figure 10c. These results provide an important and promising implication of such photocatalysts for virus disinfection in dark and indoor as well as outdoor environments. This is evidenced by the presence of virus (white spots in Figure 10d) in the digital image of active SARS-CoV-2 virus without Cu_xO/TiO_2 photocatalysts while when the photocatalysis was conducted under visible light irradiation using a white fluorescence bulb, no virus was seen (Figure 10e [73]). It is evident that the TiO_2 coating could be a potential nanomaterial for limiting the virus spread in poorly ventilated as well as in high-traffic public places [28,74,77].
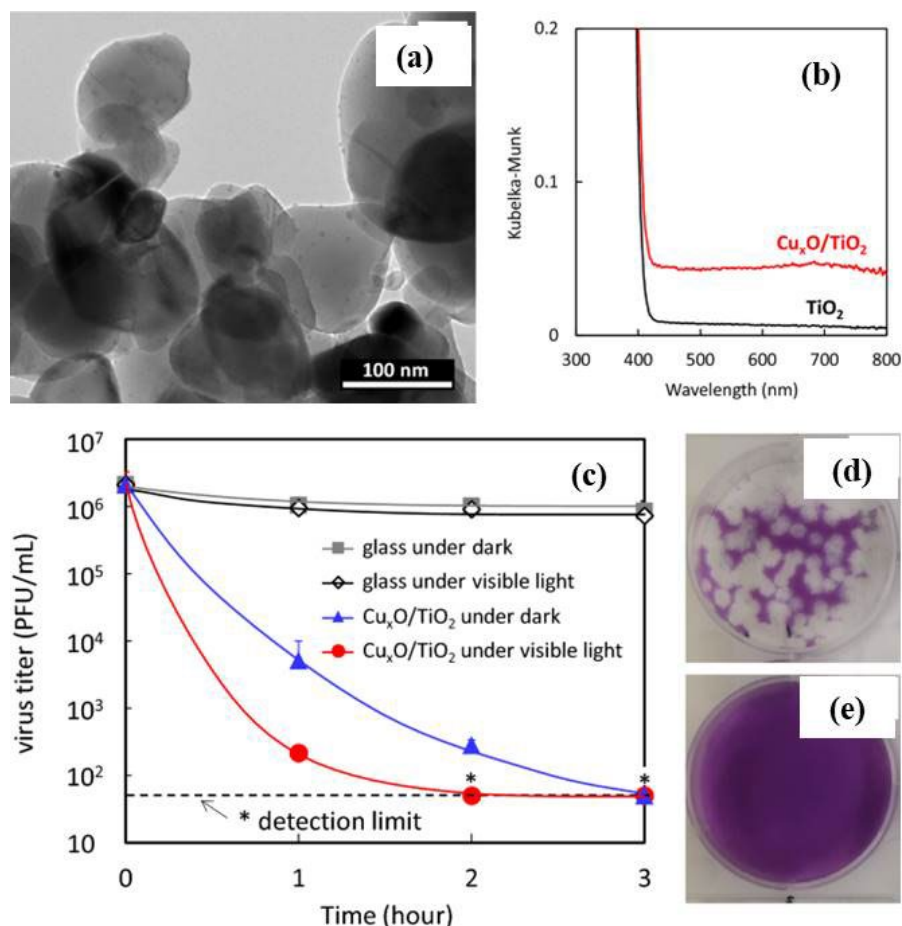
Figure 10. (**a**) Morphology of Cu_xO/TiO_2 and (**b**) UV–Vis spectra of $CuxO/TiO_2$ showing the visible light active photocatalyst. Inactivation of wild-type strain of SARS-CoV-2 by photocatalyst; (**c**) experimental results of inactivation of virus titer of SARS-CoV-2; photograph of (**d**) viral plaques infected by SARS-CoV-2 without photocatalyst; and (**e**) viral plaques infected by SARS-CoV-2 for $CuxO/TiO_2$ photocatalyst under visible light irradiation [73].

3.2. ZnO Based Nano-Photocatalysts as Potential Antibacterial and Antiviral Agents

Zinc oxide (ZnO) is the most capable wide band gap (3.37 eV) semiconductor inorganic material with a broad range of applications in the field of sensors, UV laser, photocatalysis and photovoltaics [79]. ZnO have also been used in different biological and environmental applications. The food and drug administration of United States has already provided the safety confirmation about ZnO [80]. Many biological applications of ZnO have been reported by the research in the field of biosensors, glucose, biomedical imaging, estimations of enzyme, etc. [81]. Particularly, as a potential antibacterial and antiviral agent, ZnO shows promising disinfection activities due to the creation of ROS and zinc ions which leads to the cell membrane disintegration, cell lysis, membrane protein damage, resulting in cell death [82]. The largely valuable antibacterial mechanism is the production of ROS, which is

directly related to cell death by damaging functional cellular components, such as proteins and DNA.

As discussed in the last section, use of nano-photocatalysts in environmental disinfection is promising for the health of society and can be achieved by producing efficient nanomaterials with excellent antimicrobial and antiviral agents that can work in disinfecting air, water and common surfaces [83]. ZnO is another highly researched nano-photocatalysts which has been investigated in previous years during the pandemic period for such purposes in the environmental and healthcare applications. The ZnO based nanostructures have been modified by different approaches such as tailoring of size, surface modifications by doping, annealing, or forming heterojunctions [12,19,23,84–86] for making an efficient antimicrobial, and antiviral nanomaterials. For example, Silva et al. [19] reported that the surface modification of the ZnO NPs using (3-glycidyloxypropyl) trimethoxy silane which allowed the dispersion of ZnO NPs in water providing an important pathway for uniform water disinfection without further contamination. Similarly, use of ZnO NPs was demonstrated for the bacterial decontamination on the surfaces as well as in drinking water, remotely, and most importantly, in the absence of sunlight by Milionis et al. [85]. ZnO based superhydrophobic, and self-cleaning surfaces were prepared by depositing highly conformal, biodegradable, and water-soluble fluoroalkylsilane (FAS) or ethanol-soluble stearic acid (SA) as shown in Figure 11a–c. The low bacterial adhesion was recorded on superhydrophobic ZnO substrates due to the self-cleaning properties. Hence, inhibition of surface bacterial contamination was observed. The wetting properties were studied using contact angle measurements as shown in Figure 11a. It was found that optimal concentrations for SA and FAS resulted in advancing contact angle (ACA) of 160° and CAH of 5° for the case of SA and ACA of 158° and contact angle hysteresis (CAH) of 3° for the FAS and corresponding morphologies were studied with SEM micrographs shown in Figure 11b (SA) and Figure 11c (FAS). Mechanism of interaction with ZnO nanostructures with microbes was proposed as shown in Figure 11d–e. When microbes were in contact with the ZnO surface, antibacterial action took place through the released zinc ions (Zn^{2+}) and ROS as shown schematically in Figure 11d(i,ii). When interaction took place with superhydrophilic ZnO nanostructures, due to the sharp edges of the ZnO nanostructures via killing mechanism puncturing of the cell walls occurred as shown in Figure 11d(iii). These mechanisms of antibacterial actions of ZnO nanosctures on *E. coli* are shown in SEM micrographs on different surfaces as shown in Figure 11e(i–iii). They applied these ZnO superhydrophilic surfaces in inactivation of *E.coli* in water disinfection under static and shaking conditions as shown in Figure 11f–g. It was found that these ZnO nanostructures showed the highest efficacy.

The size and concentration change of the ZnO NPs are another important factors which influence the antimicrobial/viral activities. The smaller sizes are more effective and promising antimicrobial agents, however, the structural differences in various pathogens are also important to consider the effectiveness of the NPs. Raj et al. [84] studied the disinfection activities with emphasis on effect of size and concentration of ZnO NPs on microbes with different structures. It was found that the bacterial strains are important factor and due to the structural differences between *E. coli* and *P. aeruginosa*, the antibacterial efficiency of ZnO NPs was also not same. It was also found that the zone of inhibition was increased with increasing the concentration and decreasing the size of ZnO NPs. The smaller ZnO NPs showed better bactericidal activity whereas the larger NPs presented the bacteriostatic activity. The doped ZnO nanostructures show enhanced properties such as surface area and charge transfer which are beneficial for the disinfection activities. A number of investigations have been carried out on doped ZnO with an emphasis on improving its surface, optical and charge transport properties for particularly photocatalysis and antibacterial activities [87–89]. These all contribute to the production of greater ROS which enhances disinfection activities. Naskar et al. [90] reported that the antibacterial activity of ZnO NPs was improved with Ni doping because of the increased surface area and decreased crystallite size. The morphological changes occurred in multidrug-resistant

strains of *E. coli* and *A. baumannii* were investigated by SEM technique before and after exposure to 5% Ni doped ZnO (NZO) as shown in Figure 12a–d. It can be seen in the SEM micrographs that untreated *E. coli* and *A. baumannii* cells are with smooth and intact surfaces (Figure 12a,c respectively). However, variations in morphologies of the cells were observed as a result of membrane corrugations after treatment with 5% doped NZO due to wrinkling and damaging of the cell membranes as shown by red circles indicating the areas of cell membrane disruption (Figure 12b,d corresponding to the Figure 12a,c respectively). The 5% doped NZO NPs demonstrated better antibacterial activity with respect to other concentration which was attributed to the high production of ROS which was studied and quantified using fluorescence intensity at 520 nm of *E. coli* ATCC 25922 cells as shown Figure 12e.
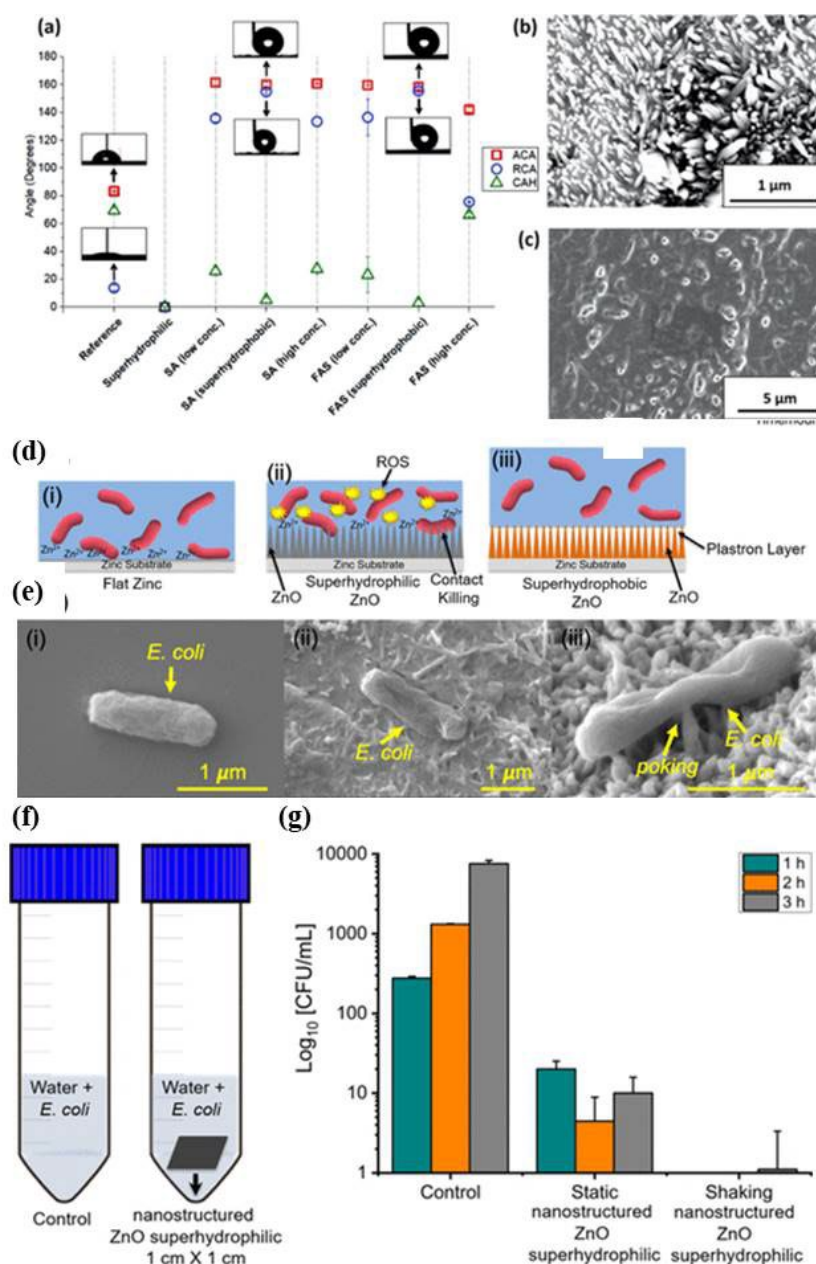
Figure 11. (**a**) Wetting properties using contact angle measurements done for different ZnO based samples. SEM micrographs of: (**b**) SA-coated; (**c**) FAS-coated ZnO nanostructures; (**d**) schematic

representation mode of interactions of surface–bacteria on flat Zn substrates, nanostructured superhydrophilic ZnO surfaces, and nanostructured hydrophobized ZnO surfaces; (**e**) SEM micrographs of E. coli on (i) glass coverslip, (ii) flat zinc, and (iii) nanostructured ZnO superhydrophilic surface; and (**f,g**) ZnO superhydrophilic surfaces in inactivation of E.coli in water disinfection under static and shaking conditions. (reproduced with permission from Ref. [85] copyright-2020 American Chemical Society).
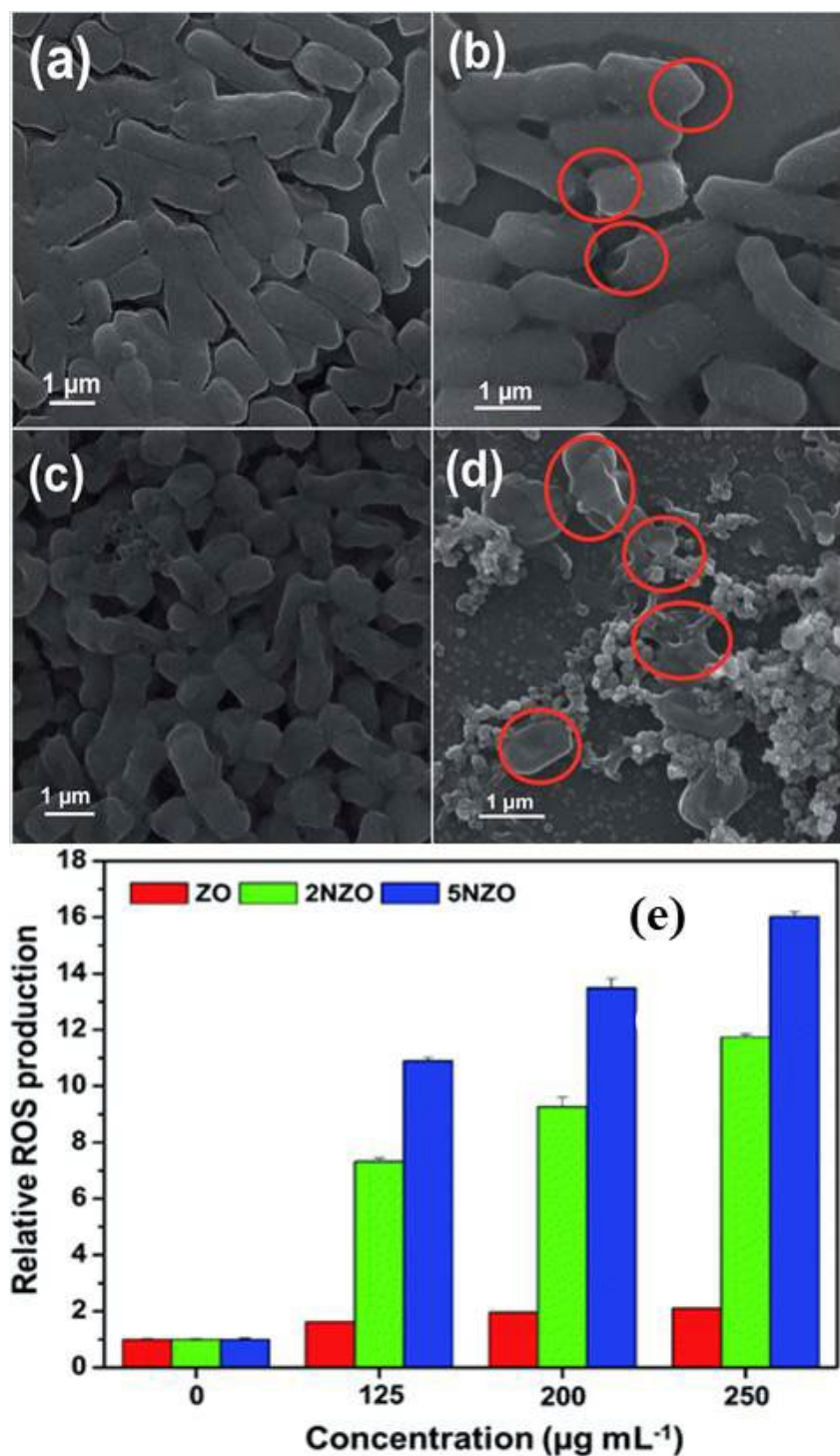
Figure 12. The surface morphology of bacterial cells: (**a**) untreated samples of *E. coli*; (**b**) treated sample of *E coli* by 5% doped NZO; (**c**) untreated samples of *A. baumannii;* (**d**) treated samples of *A. baumannii* with 5% doped NZO; and (**e**) quantification of ROS production using fluorescence dye [90].

Stability of such functionalized ZnO nanostructures is one of the important concerns for real practical applications. In this context, different approaches have been applied. For example, concerning air pollution with bacterial contaminants which really causes several type of health problems, Geetha et al. [91] produced stable and low cost ZnO nanofibers based polymer nanocomposites as a promising coating for face masks, with an aim to filter both particulate and bacterial contaminants. ZnO NPs were dispersed homogeneously in the mixed PVA/PVP polymer blend solution and using electrospinning system, ZnO nanofilbers-polymer nanocomposites were produced with different ZnO NPs concentrations as shown in Figure 13a–d. Figure 13a Shows the SEM micrographs of the ZnO NPs which are agglomerated having NPs of different sizes. The morphology of the only polymer nanofibers shows uniform and smooth morphology as shown in Figure 13b. Whereas, ZnO based polymer nanocomposites are shown in Figure 13c,d which exhibit rough surface morphology attributed to the embedded ZnO NPs. ZnO based polymer nanofibers are also shown to be of increased size attributed to the increased concentration of ZnO NPs. Several bacteria were treated with these ZnO based polymer nanocomposites and their antibacterial effects were studied. The microbial growth inhibition efficiency of ZnO NPs, only polymer, and ZnO-polymer nanocomposite fibers for the *S. aureus*, *E. coli*, *K. pneumonia* and *S. aeruginosa* bacteria are shown in Figure 13e. It was found that around the electrospun circular mask, there was no bacterial growth observed for a particular distance when nanocomposite was applied with different concentration of ZnO NPs in nanocomposites to the mask, whereas there was no any disinfection/inhibition zone effect observed for only polymer nanofibers. These results show good results, indicating the usefulness of the prepared nanofibrous material for antimicrobial face masks as shown in Figure 13f.
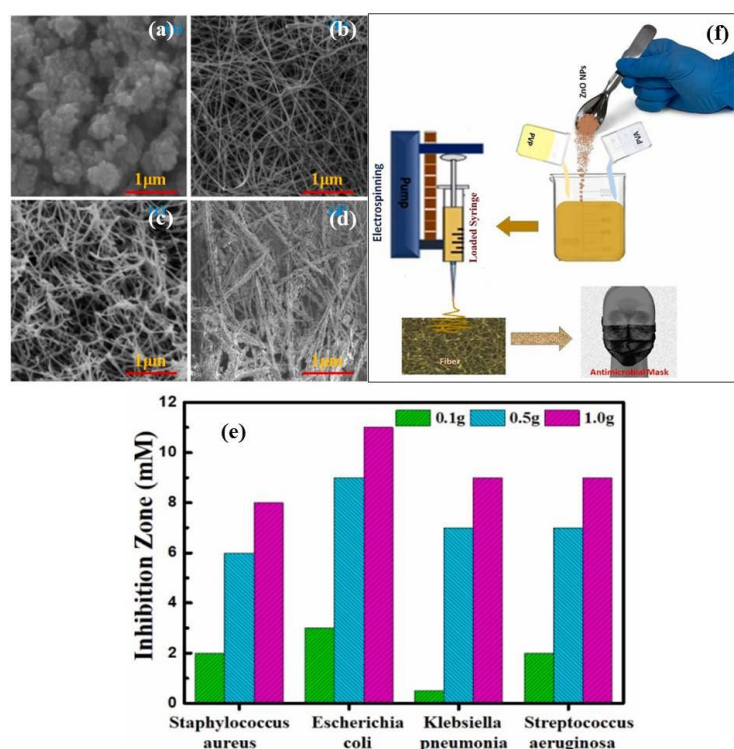
Figure 13. SEM micrographs of (**a**) ZnO NPs; (**b**) PVA/PVA; (**c**) ZnO (0.1 g)/PVA/PVP; (**d**) ZnO (1 g)/PVA/PVP composites; (**e**) the microbial growth inhibition efficiency of ZnO/PVA/PVP nanocomposite fiber against *S.aureus*, *E. coli*, *K. pneumonia* and *S. aeruginosa;* and (**f**) schematic of synthesis of ZnO-polymer based composite nanofibers for the application of face mask (eproduced with permission from Ref. [91]. Copyright 2022-Elsevier).

ZnO NPs are exploited as promising antiviral nanomaterials against different kind of viruses including SARS-CoV-2 [83,92]. ZnO NPs have been used against herpes simplex virus type 111 and H1N1 influenza virus [93–97]. Usually, zinc is an important element that observed in bone, muscle, brain, and skin of human. This vital element is also concerned in different enzyme processes like protein and metabolism [98]. Zn is observed to impede both SARS-CoV and retrovirus in vitro RNA polymerase activity, as well as zinc ionophores which hinder the viruses replication in cell culture [99]. Zn was also established to reduce the viral replication of different RNA viruses like respiratory syncytial virus influenza virus, and numerous picornaviruses [97,100]. ZnO NPs show better performance in antiviral activity as compared to the other antiviral materials because they have also emanated from their good compatibility to biological systems, high safety, low price, and good stability [101]. Additionally, visible fluorescence of ZnO is used in bioimaging and control monitoring of the drug. All the premises of ZnO NPs presented show potential in the design of nanomedical viral-targeting therapies.

Hamdi et al. [93] reported that ZnO could be used for vitro characterizations and cellular uptakes in human lung fibroblast cells and then proposed a mechanism of ZnO against COVID-19. They synthesized ZnO NPs and studied its surface, structural and morphological properties in view of its interaction with virus. The estimation of surface charge of ZnO NPs was found to be important to understand the interaction with the biological membranes. The value of zeta potential for optimized ZnO NPs was recorded from +25.32 to −18.78 and found to be highly dependent on the dispersant medium pH. The release profiles of Zn^{2+} at different pH was optimized and it was found that higher Zn^{2+} solubility in the acidic medium was the reason for the higher Zn release at pH 5.5. In silico molecular docking was investigated to speculate the possible interaction between ZnO NPs and COVID-19 targets including the ACE2 receptor, COVID-19 RNA-dependent RNA polymerase, and main protease. Interestingly, felicitous binding of these ZnO NPs with the three tested COVID-19 targets, via hydrogen bond formation, was observed and an enhanced dose-dependent cellular uptake was proposed. The proposed mechanism of interaction of ZnO NPs with SARS-CoV-2 has been shown schematically in Figure 14.
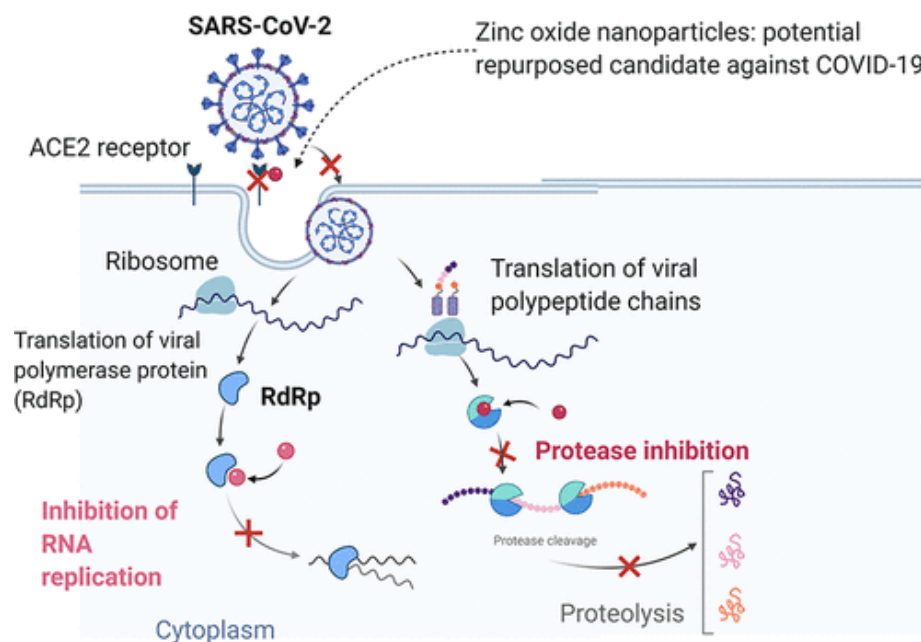

Figure 14. Schematic of interaction of ZnO NPs with SARS-CoV-2 [93].

3.3. CuO and Other Metal Oxides Based Nano-Photocatalysts as Potential Antimicrobial and Antiviral Agents

Due to their narrow band structure and open surface sites, structurally modified inorganic metals NPs and their oxide forms possess special physical and chemical characteristics that make them more suitable to interact with pathogens and microorganisms. In this regard, a number of antiviral medicines made of transitional metal-oxide such as ZnO, CuO, and TiO_2 were found. It has been discovered that after entering the host cells, viruses attach, invade, duplicate, and branch out. While the antiviral properties of the metal-based nanomaterials may interact with the virus to restrict the insertion of the virus into the cell body. Additionally, the metal-oxides generate extremely potent free radical species that damage the nucleus of the virus and prevent it from killing the organelles of living cells.

Due to its functionalized surfaces and electronic band structures, CuO has been investigated as an antibacterial and antiviral agent among the many metal oxides [102–104]. As one of the most effective nanocatalysts for fighting bacteria, fungus, and viruses at the right concentration, it is also one of the least poisonous and expensive nanomaterials [103]. The antimicrobial activity of CuO NPs is due to their close interaction with bacterial membranes and the release of metal ions. When the NPs are near the lipid membrane, they slowly oxidize, release copper ions, and generate harmful hydroxyl free radicals. These free radicals separate the lipids from the cell membrane through oxidation and destroy the membrane [105]. The entire genome order of the virus is frequently destroyed in the nuclei by these reactive ions or radicals [106]. Mechanistically, the free radical ions damage the host's proteins, lipids, and viral glycoproteins in the outermost receptor surface. The damaged cell membranes (coenzyme A) therefore, disrupted metabolic processes (respiration), leading to cell lysis or virus destruction [107,108]. Consequently, in the case of CuO, the free Cu ions produced from Cu_2O/CuO inspire the formation of free radicals that prompt the destruction of the outer capsid level of the virus. It eventually destroys their genomic sequences and the replication process is stopped at a non-cytotoxic amount [109]. In order to remove organic pollutants and different pathogens from waste water, it has also been employed as a better photocatalyst [110,111]. The band gap of CuO is ~1.7 eV [110]. It has demonstrated excellent promise for use in the creation of antibacterial compounds as well as the photocatalytic destruction of organic contaminants. For instance, Akhavan et al. [112] showed that the Cu and CuO NPs covering had antibacterial action both in the dark and when exposed to light.

The information above demonstrates the potential of CuO NPs to function as effective antibacterial or antiviral agents in indoor or outdoor settings, i.e., in the absence of sunshine or underwater. A composite coating made of Cu_2O NPs and linear low-density polyethylene, for instance, showed antibacterial characteristics for the disinfection of water as studied by Gurianov et al. [113]. The composite exhibited no or very low leaching of copper ions into the aqueous phase, showing good antibacterial activity against *S. aureus* and *E. coli*. Similarly, Domagala et al. [114] investigated the antiviral effectiveness of Cu_2O nanostructures encapsulated on multi-walled carbon nanotubes (MWCNTs) based filters and their stability for virus removal from water. Three different procedures were followed to produce different nanocomposites with MWCNTs such as (1) direct Cu ion attachment, (2) $Cu(OH)_2$ extraction, and (3) $[Cu(NH_3)_4]^{2+}$ complex bonding with MWCNTs. The formation of nanocomposites and distribution of Cu_2O on MWCNTs were confirmed by TEM images as shown in Figure 15a–c. The MS2 bacteriophages elimination assays were carried out twice, once before (day 1) and again (day 2) post treating filters using water at pH of 5 and 7. (24 h) as shown in Figure 15d,e. The effective removal outcomes showed how important the methodology is for the removal of viruses, the efficiency of disinfection in Cu_2O-coated MWCNTs, and the potential for virus elimination due to copper's antibacterial capabilities as well as retaining viral electrostatic adsorption in MWCNTs. Similarly, Mazukow et al. [115] developed a spray based on alumina granules deposited with CuO NPs filters for virus removal from water as schematically depicted in Figure 15f and also investigated the effect of copper oxidation state on virus removal capacity. It was found that

an alumina support of this kind offered a porous structure to ensure extended interaction with water-harbouring viruses. It was discovered that the principal virus-removing phases were copper (I) oxide and metallic copper, and 99.9% of MS2 bacteriophages could be eliminated [115].

Antimicrobial property of thermocycled polymethyl methacrylate denture base resin reinforced with CuO NPs was studied by Giti et al. [104]. The CuO NPs may also be effective as a potential control agent or candidate for avoiding dental infections or caries [116]. In a study, it was found that CuO NPs doped with Fe were effective against biofilm forming bacteria and fungi [103]. These Fe doped CuO NPs showed better photocatalytic and antimicrobial efficacy because of reduced band gap of 1 eV. By co-culturing CuO NPs with HSV-1-infected cells at a certain concentration of CuO NPs (100 g/mL), Ahmad Tavakoli and colleagues [109] showed that the CuO NPs had excellent anti-HSV-1 viral efficacy. This disinfection level of the cell was subsequently increased to 83.3%. ROS were discovered to be mostly produced by semiconducting CuO NPs, which were then bound to the HSV-1 and destructed the virus's DNA. The HCV was also discovered to be resistant to Cu_2O NPs [117] (Figure 15g–k). According to this study, Cu_2O NPs exhibited inhibitory effect on virus infection on the target cells by blocking the virus infection both at the attachment and entry stages.
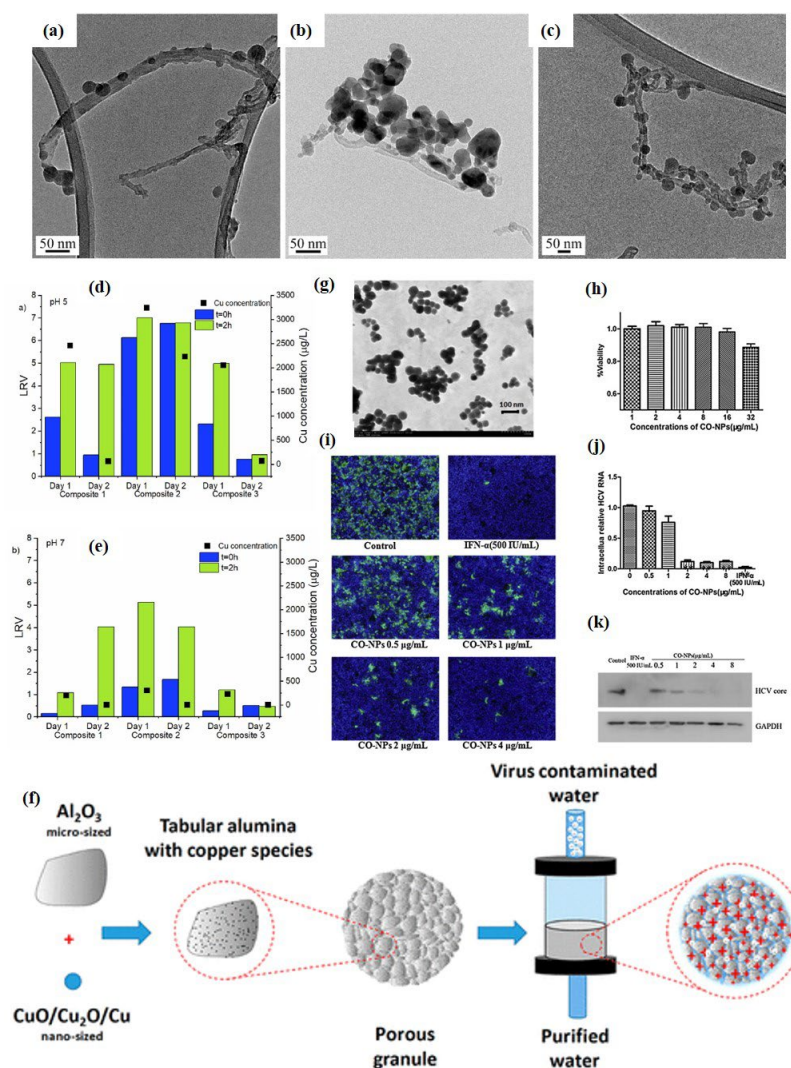

Figure 15. TEM images of Cu_2O-MWCNTs nanocomposites: (**a**) composite 1; (**b**) composite 2; (**c**) composite 3. MS2 removal test results for composite 1, composite 2 and composite 3 at (**d**) pH 5

and (**e**) pH 7, and the associated copper concentrations detected in the permeate (reproduced with permission from Ref. [114] Copyright 2020-Elsevier); (**f**) Schematic representation of nano-sized copper (Oxide) on alumina granules filters for water filtration. Reproduced with permission from Ref. [115] Copyright 2020, American Chemical Society. Cu_2O (CO) NPs inhibited HCV infection. HCVcc (MOI = 0.1) virions were added with the indicated concentrations of Cu_2O NPs or interferon-(IFN-, 500 IU/mL) to Huh7.5.1 cells. After incubation at 37 °C for 2 h, the cells were washed three times to remove the virus and treated with the indicated concentrations of Cu_2O NPs for additional 72 h; (**g**) the TEM image of Cu_2O NPs; (**h**) Huh7.5.1 cells were treated with Cu_2O NPs at the indicated doses for 72 h. The effect of Cu_2O NPs on cell viability was measured by a CCK8 assay kit; (**i**) Huh7.5.1 cells at 72 h post-infection were stained with HCV-positive serum from patients and with DAPI. Representative fluorescence images are shown (80× magnification); (**j**) The intracellular HCV RNA content was determined by qRT-PCR; and (**k**) Western blot analysis of the harvested cell lysates using the anti-core or anti-GAPDH antibodies. Results are represented as the mean ± SD from 3 independent experiments ($p < 0.001$) (reproduced with permission from Ref. [117]. Copyright 2015-Elsevier).

The aforementioned examples demonstrate the potent antiviral and antibacterial characteristics of CuO and Cu_2O NPs, as well as how these properties can be maintained even when embedded in layers of polymeric covering. This may hold promise for effective real-world applications against viral and microbial diseases on surfaces used for public usage. Without altering the mask's standard filtration procedure, Borkow et al. [118] demonstrated that CuO impregnated masks could be helpful in lowering the danger of pathogen transmission/contamination in the air. It was proposed that such masks containing CuO NPs also provide protection from any kind of pathogens and are very important for combatting against the spread of and infection by dangerous pathogens attributed to the potent antiviral and antibacterial properties of CuO. As shown in Figure 16a–c [118], a respiration face mask was prepared containing CuO as an antiflu treatment. It was found that these CuO containing masks effectively filtered more than 99% of inhalational influenza viruses such as H1N1 and the H9N2. Very recently, Leung et al. also proved a high efficacy of CuO NPs decorated respiratory masks that efficiently decrease viral infections [119].
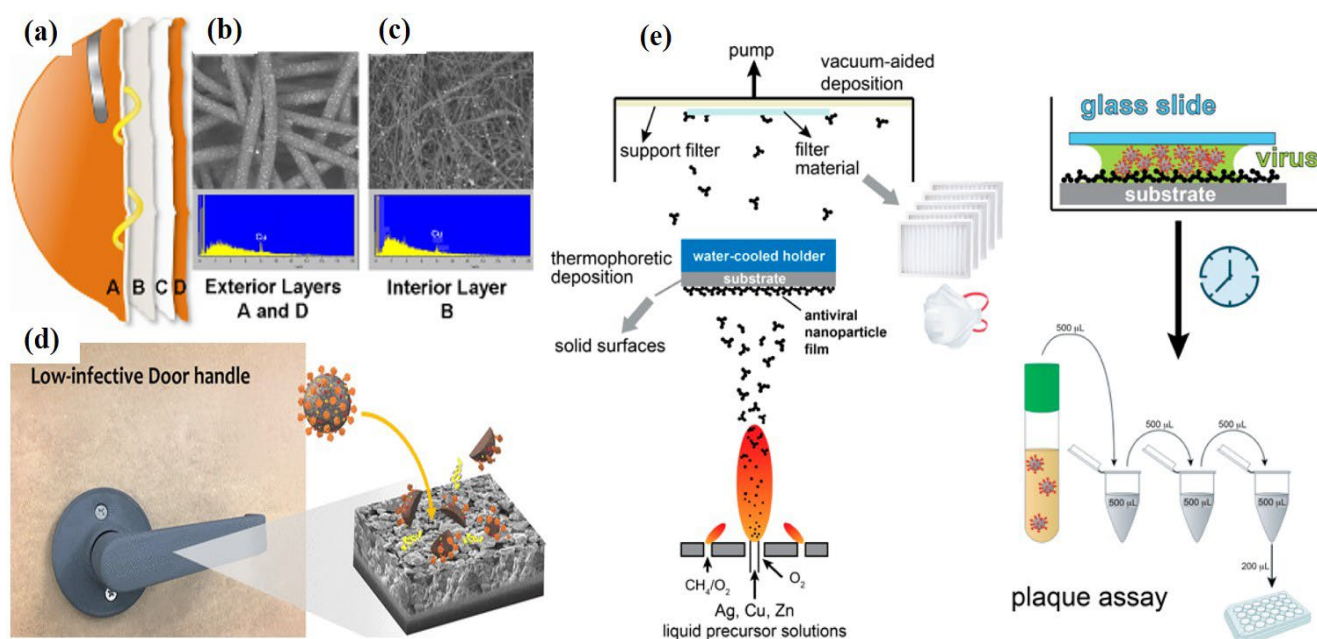

Figure 16. (**a**) CuO impregnated masks; (**b**) outer coating of mask covering CuO NPs; (**c**) inner coating of mask covering CuO NPs. [118]; (**d**) schematic of cupric Oxide coating on the common

surfaces such as door locks that rapidly reduces infection by SARS-CoV-2 (reproduced with permission from Ref. [120] Copyright 2021-American Chemical Society); and (**e**) schematic of the flame aerosol deposition process of antiviral nanoparticle coatings on solid flat substrates as well as on porous filter materials. The as-prepared nanoparticle coatings are then incubated with SARS-CoV-2, and their antiviral activity is examined by the plaque assay [121].

The primary cause of the coronavirus illness, COVID-19, is the SARS-CoV-2 virus, which spreads through repeated contact or aspiration of respiratory secretions. CuO and Cu_2O are ionic forms of the Cu ions, and their antiviral, antifungal, and antibacterial properties imply that they may also be useful against the SARS-CoV-2 virus. The effects of a Cu_2O coating on a SARS-CoV-2 virus disseminated solution in an aqueous droplet were investigated by Hosseini et al. [120]. In the experiment, they used a live SARS-CoV-2 strain rather than a proxy virus on BSL-3 environments. It was discovered that the developed coating was quite helpful in reducing COVID-19 transmission and contacting concerns. To reduce disease transmissions, the cost-effective and stable coating was created and applied to places where the public can touch, like door handles (Figure 16d). The Cu_2O NPs were compacted into a strong coating followed by thermal annealing which allows forming the crystalline solid phase of CuO crystals. The CuO coated on SARS-CoV-2 infectivity was lowered by 99.8% in 30 min and then 99.9% in an hour, while the coating stayed hydrophilic for around 5 months. Merkl et al. [121] investigated the effect of antiviral coating of various nanomaterials such as Ag, CuO and ZnO by depositing on both solid flat surfaces as well as porous filter media. The antiviral studies were carried out against SARS-CoV-2 viability and were compared with a viral plaque assay. The coatings were prepared by aerosol nanoparticle self-assembly during their flame synthesis as shown in Figure 16e. It was found that as compared to ZnO, other coatings were more effective including CuO showing their potential as antiviral coatings on variety of surfaces to reduce the transmission of viruses. Recently, Delumeau et al. [122] demonstrated that Cu and Cu_2O thin-film coatings deposited on glass had very strong antiviral effect on human coronavirus HCoV-229E. Additionally, the coating was placed to a N95 mask, and it was discovered through droplet studies that the coating decreased viral infectivity by 1–2 orders of magnitude in just over an hour.

In addition to everything mentioned above, CuO has demonstrated superior antiviral and antimicrobial photocatalyst properties, as well as being a better supporting material to increase the photocatalytic disinfection efficiency of other wide band gap photocatalysts like TiO_2 NPs in both indoor and outdoor environments [123]. Inactivation of various variant types of SARS-CoV-2 by indoor-light-sensitive TiO_2-based photocatalyst [110]. For example, Farah et al. [123] studied the *E. coli* disinfection in indoor air under the photoreactor and found that CuO-TiO_2 nanocomposite acted as excellent photocatalyst. Nakano et al. [73] studied antiviral behaviour of Cu_xO/TiO_2 photocatalyst under the indoor light environment and found the excellent antiviral effect against COVID-19. Kanako et al. [124] demonstrated the photocatalytic antibacterial activity of TiO_2, TiO_2 + CuO, and WO_3 + CuO and found that composite with CuO enhanced the photocatalytic antibacterial activity of TiO_2 and WO_3 photocatalysts. In addition, WO_3 has been investigated for its potential photocatalytic properties for disinfection activity [125,126]. It is an n-type semiconductor capable of absorbing the visible light up to 480 nm (bandgap energy ranges between 2.5–3.0 eV) with an excellent photostability and surface transport properties [127]. The potential application of WO_3 based nano-photocatalyst coating in inactivation of SARS-CoV-2 under the visible light was demonstrated by Uema et al. [125] in different environmental conditions. A low-cost multiphase photocatalyst from industrial waste and WO_3 was proposed by Hojamberdiev et al. [127] for photocatalytic removal of SARS-CoV-2 antiviral drugs (lopinavir and ritonavir) in real wastewater for practical applications.

4. Challenges, Future Prospects and Summary

In conclusion, this paper provides a concise overview of the research background and significance of recent advances in metal oxide-based nano-photocatalysts as potential antimicrobial and antiviral agents. Emphasis is placed on understanding photomechanism processes and potential applications in the outdoor and indoor environment including water and air contamination [128]. To advance current technologies, many research groups have focused on the development of new photoreactors based on metal oxides. Using nanomaterial components not only enables more efficient and speedier regulation of the spread of dangerous viruses such as H1N1, SARS-CoV, and SARS-CoV-2, but also tends to make protective masks, fabrics, and screens reproducible in community settings. More research into the antiviral properties of transition metal oxides is required to reduce the severity of viral infections and prevent potential pandemics. As a result, it is reasonable to assume that in the coming years, such novel transitional metal oxide photocatalysts will undoubtedly pave the way toward an effective way to completely overcome the dangerous SARS-CoV-2. Metal oxide semiconductor photocatalysts have been extensively investigated for their ability to inactivate a variety of viruses and microorganisms. Examples of these photocatalysts include TiO_2 and ZnO. The photocatalytic inactivation of microorganisms is a synergistic bactericidal and virucidal effect of electromagnetic radiation at a given wavelength and the oxidative radicals produced by the photocatalyst when exposed to UV light. In this context, TiO_2 has been the subject of extensive research and has been successfully implemented in various well-known disinfection technologies. The crystallinity and concentration of the photocatalyst, as well as the appropriate combination of the intensity of the light applied, and the irradiation time, play a major role in determining the efficiency of UV-induced TiO_2 photocatalysis. The efficiency is a function of several parameters.

At present copper oxide impregnated masks safely reduce the risk of influenza virus environmental contamination without altering the filtration capacities of the masks. Due to the potent antiviral and antibacterial properties of copper oxide, we believe that these masks also confer protection from additional pathogens, and, as such, are an important additional armament in the combat against the spread of and infection by dangerous pathogens. The production of the mask layers with copper oxide and the manufacture of the mask using these materials do not add any significant costs to the price of the masks. It is suggested that copper oxide should be also included in other personal protective equipment to further confer protection to the wearer and to the environment [118]. Pathogens and certain other infectious germs cannot enter the wearer's nose or mouth using defensive breathing face masks. Nevertheless, improper handling and maintenance of masks, particularly when they are used by non-professionals like the common person, could probably induce pathogen transmission. The ROS-based concepts have already been reported by several different types of studies for the improved antibacterial and antifungal properties using semiconducting metal oxides nanomaterials. This improvement is attributed to the fast productions of ROS and the slow recombination rate of the electron-hole charges in the nanomaterials. Therefore, to reduce the spread and infections of viruses like SARS-CoV-2, numerous reasonable precautions including antiviral medications, passive vaccination, many antiseptic solutions, UV irradiation, antibodies are in practice [129–131].

As a result, CuO might find use in medical research and in the design of healthy environments in the form of NPS, thin films, or functionalized nanostructures. Overall, the semiconducting metal-oxides (photocatalyst) like CuO, TiO_2, and ZnO have been appreciated for enhanced antiviral activities due to their structural, optical, and surface engineering at the nanoscale. The best method for inactivating encapsulated viruses is thought to be photocatalytic nanomaterials, which need illumination as their power source. Therefore, photocatalytic reactions take place because of a cumulative impact of solar energy at a fixed frequency and the photoactive substance, which captures a diverse range of sunlight wavelengths. These could be more practically applicable for the betterment of society and the environment.

5. Challenges

1. Due to the wide bandgap that it possesses, natural TiO_2 can only be excited by the near-UV photons that are present in the solar spectrum (390 nm). However, visible light accounts for approximately 42% of solar radiation [132], despite the fact that UV makes up only 4% of solar light. Because of its wide bandgap, it is not useful for applications involving the environment. As a result, boosting the photocatalytic activity of TiO_2 is a difficult problem;

2. It is common knowledge that photocatalytic nanomaterials could generate ROS, which can then destroy the structural components of viruses. However, the light source has a significant impact on their performance, which may result in an increase in the cost of their application;

3. It is important to tailor the development and choice of antiviral nanomaterials to their intended uses. The high flow rate of air purifiers makes it easier for viruses to gain momentum when antiviral materials are used. Because of this, nanomaterials' electrostatic effects on their surfaces should be amplified to improve their adsorption capacities toward viruses, and their physical structures should be strengthened to break viruses;

4. The biodistribution of metal oxide NPs is influenced by their interactions with proteins, which take place through a process known as opsonization. As a result, the NP's properties are altered [133];

5. When metal NPs are utilized for in vivo applications, it is imperative that the potentially harmful effects of these particles be taken into consideration. Nanotoxicity can be explained by two factors: (i) the potential release of toxic ions from metallic nanoparticles, and (ii) the oxidative stress caused by the inherent properties of the nanoparticles themselves (morphology, surface charge, size, and chemical surface composition) [134].

To sum up, it is crucial to integrate the safety assessment of the metal oxide-based nano-photocatalysts from the earliest stages of material design, synthesis, and development in order to implement the full potential of antimicrobial or antiviral nanomaterials, to consider both environmental and human health risks at each stage of the product life cycle, and, as is especially important, in the case of antibacterial nanomaterials, to consider the potential exposure effects on human commensal microorganisms. Many nanomaterials used to treat bacterial infections also have antiviral properties, so studying them could lead to novel approaches in treating and preventing the spread of viruses.

Conflicts of Interest: The authors declare no conflict of interest.

References

1. Prakash, J.; Cho, J.; Mishra, Y.K. Photocatalytic TiO2 nanomaterials as potential antimicrobial and antiviral agents: Scope against blocking the, SARS-CoV-2 spread. *Micro Nano Eng.* **2022**, *14*, 100100. [CrossRef]
2. Soni, V.; Khosla, A.; Singh, P.; Nguyen, V.-H.; Van Le, Q.; Selvasembian, R.; Hussain, C.M.; Thakur, S.; Raizada, P. Current perspective in metal oxide based photocatalysts for virus disinfection: A review. *J. Environ. Manag.* **2022**, *308*, 114617. [CrossRef] [PubMed]
3. Guerra, F.D.; Attia, M.F.; Whitehead, D.C.; Alexis, F. Nanotechnology for Environmental Remediation: Materials and Applications. *Molecules* **2018**, *23*, 1760. [CrossRef] [PubMed]
4. Talebian, S.; Wallace, G.G.; Schroeder, A.; Stellacci, F.; Conde, J. Nanotechnology-based disinfectants and sensors for, SARS-CoV-2. *Nat. Nanotechnol.* **2020**, *15*, 618–621. [CrossRef]
5. Aghalari, Z.; Dahms, H.-U.; Sillanpää, M. Investigating the effectiveness of nanotechnologies in environmental health with an emphasis on environmental health journals. *Life Sci. Soc. Policy* **2021**, *17*, 8. [CrossRef]

6. Soliman, A.M.; Khalil, M.; Ali, I.M. Novel and Facile Method for Photocatalytic Disinfection and Removal of Organic Material from Water Using Immobilized Copper Oxide Nano Rods. *J. Water Process Eng.* **2021**, *41*, 102086. [CrossRef]

7. Chakraborty, A.; Samriti Ruzimuradov, O.; Gupta, R.K.; Cho, J.; Prakash, J. TiO$_2$ nanoflower photocatalysts: Synthesis, modifications and applications in wastewater treatment for removal of emerging organic pollutants. *Environ. Res.* **2022**, *212*, 113550. [CrossRef]

8. Samriti, M.; Chen, Z.; Sun, S.; Prakash, J. Design and engineering of graphene nanostructures as independent solar-driven photocatalysts for emerging applications in the field of energy and environment. *Mol. Syst. Des. Eng.* **2022**, *7*, 213–238. [CrossRef]

9. Prakash, J.; Sun, S.; Swart, H.C.; Gupta, R.K. Noble metals-TiO$_2$ nanocomposites: From fundamental mechanisms to photocatalysis, surface enhanced, Raman scattering and antibacterial applications. *Appl. Mater. Today* **2018**, *11*, 82–135. [CrossRef]

10. Gupta, T.; Cho, J.; Prakash, J. Hydrothermal synthesis of TiO$_2$ nanorods: Formation chemistry, growth mechanism, and tailoring of surface properties for photocatalytic activities. *Mater. Today Chem.* **2021**, *20*, 100428. [CrossRef]

11. Prakash, J.; Kumar, P.; Harris, R.A.; Swart, C.; Neethling, J.H.; van Vuuren, A.J.; Swart, H.C. Synthesis, characterization and multifunctional properties of plasmonic Ag–TiO$_2$ nanocomposites. *Nanotechnology* **2016**, *27*, 355707. [CrossRef]

12. Singh, N.; Prakash, J.; Gupta, R.K. Design and engineering of high-performance photocatalytic systems based on metal oxide–Graphene—Noble metal nanocomposites. *Mol. Syst. Des. Eng.* **2017**, *2*, 422–439. [CrossRef]

13. Rajput, V.; Gupta, R.K.; Prakash, J. Engineering metal oxide semiconductor nanostructures for enhanced charge transfer: Fundamentals and emerging SERS applications. *J. Mater. Chem. C* **2022**, *10*, 73–95.

14. Ahmadi, Y.; Bhardwaj, N.; Kim, K.-H.; Kumar, S. Recent advances in photocatalytic removal of airborne pathogens in air. *Sci. Total Environ.* **2021**, *794*, 148477. [CrossRef]

15. Channegowda, M. Functionalized Photocatalytic Nanocoatings for Inactivating COVID-19 Virus Residing on Surfaces of Public and Healthcare Facilities. *Coronaviruses* **2021**, *2*, 3–11. [CrossRef]

16. Saravanan, A.; Kumar, P.S.; Jeevanantham, S.; Karishma, S.; Kiruthika, A.R. Photocatalytic disinfection of micro-organisms: Mechanisms and applications. *Environ. Technol. Innov.* **2021**, *24*, 101909. [CrossRef]

17. Liu, Y.; Huang, J.; Feng, X.; Li, H. Thermal-Sprayed Photocatalytic Coatings for Biocidal Applications: A Review. *J. Therm. Spray Technol.* **2021**, *30*, 1–24. [CrossRef]

18. Kumar, P.; Mathpal, M.C.; Prakash, J.; Viljoen, B.C.; Roos, W.; Swart, H. Band gap tailoring of cauliflower-shaped CuO nanostructures by Zn doping for antibacterial applications. *J. Alloys Compd.* **2020**, *832*, 154968. [CrossRef]

19. da Silva, B.L.; Caetano, B.L.; Chiari-Andréo, B.G.; Pietro, R.C.L.R.; Chiavacci, L.A. Increased antibacterial activity of ZnO nanoparticles: Influence of size and surface modification. *Colloids Surf. B. Biointerfaces* **2019**, *177*, 440–447. [CrossRef]

20. Matsuura, R.; Lo, C.-W.; Wada, S.; Somei, J.; Ochiai, H.; Murakami, T.; Saito, N.; Ogawa, T.; Shinjo, A.; Benno, Y.; et al. SARS-CoV-2 Disinfection of Air and Surface Contamination by TiO$_2$ Photocatalyst-Mediated Damage to Viral Morphology, RNA, and Protein. *Viruses* **2021**, *13*, 942. [CrossRef]

21. Gold, K.; Slay, B.; Knackstedt, M.; Gaharwar, A.K. Antimicrobial Activity of Metal and Metal-Oxide Based Nanoparticles. *Adv. Ther.* **2018**, *1*, 1700033. [CrossRef]

22. Liaqat, F.; Khazi, M.I.; Awan, A.S.; Eltem, R.; Li, J. 15-Antimicrobial studies of metal oxide nanomaterials. In *Metal Oxide-Carbon Hybrid Materials*; Chaudhry, M.A., Hussain, R., Butt, F.K., Eds.; Elsevier: Amsterdam, The Netherlands, 2022; pp. 407–435.

23. Kumar, V.; Prakash, J.; Singh, J.P.; Chae, K.H.; Swart, C.; Ntwaeaborwa, O.M.; Swart, H.C.; Dutta, V. Role of silver doping on the defects related photoluminescence and antibacterial behaviour of zinc oxide nanoparticles. *Colloids Surf. B Biointerfaces* **2017**, *159*, 191–199. [CrossRef]

24. Zacarías, S.M.; Satuf, M.L.; Vaccari, M.C.; Alfano, O.M. Photocatalytic inactivation of bacterial spores using TiO$_2$ films with silver deposits. *Chem. Eng. J.* **2015**, *266*, 133–140. [CrossRef]

25. Park, G.W.; Cho, M.; Cates, E.L.; Lee, D.; Oh, B.-T.; Vinjé, J.; Kim, J.-H. Fluorinated TiO$_2$ as an ambient light-activated virucidal surface coating material for the control of human norovirus. *J. Photochem. Photobiol. B Biol.* **2014**, *140*, 315–320. [CrossRef]

26. Si, Y.; Zhang, Z.; Wu, W.; Fu, Q.; Huang, K.; Nitin, N.; Ding, B.; Sun, G. Daylight-driven rechargeable antibacterial and antiviral nanofibrous membranes for bioprotective applications. *Sci. Adv.* **2018**, *4*, eaar5931. [CrossRef]

27. Kumar, A.; Soni, V.; Singh, P.; Khan, A.A.P.; Nazim, M.; Mohapatra, S.; Saini, V.; Raizada, P.; Hussain, C.M.; Shaban, M.; et al. Green aspects of photocatalysts during corona pandemic: A promising role for the deactivation of COVID-19 virus. *RSC Adv.* **2022**, *12*, 13609–13627. [CrossRef]

28. Khaiboullina, S.; Uppal, T.; Dhabarde, N.; Subramanian, V.R.; Verma, S.C. Inactivation of Human Coronavirus by Titania Nanoparticle Coatings and UVC Radiation: Throwing Light on SARS-CoV-2. *Viruses* **2021**, *13*, 19. [CrossRef]

29. Tong, Y.; Shi, G.; Hu, G.; Hu, X.; Han, L.; Xie, X.; Xu, Y.; Zhang, R.; Sun, J.; Zhong, J. Photo-catalyzed TiO$_2$ inactivates pathogenic viruses by attacking viral genome. *Chem. Eng. J.* **2021**, *414*, 128788. [CrossRef]

30. Bono, N.; Ponti, F.; Punta, C.; Candiani, G. Effect of UV Irradiation and TiO$_2$-Photocatalysis on Airborne Bacteria and Viruses: An Overview. *Materials* **2021**, *14*, 1075. [CrossRef]

31. Mullenders, L.H.F. Solar UV damage to cellular DNA: From mechanisms to biological effects. *Photochem. Photobiol. Sci.* **2018**, *17*, 1842–1852. [CrossRef]

32. Prakash, J.; Samriti, K.A.; Dai, H.; Janegitz, B.C.; Krishnan, V.; Swart, H.C.; Sun, S. Novel rare earth metal–doped one-dimensional TiO$_2$ nanostructures: Fundamentals and multifunctional applications. *Mater. Today Sustain.* **2021**, *13*, 100066. [CrossRef]

33. Cai, T.; Liu, Y.; Wang, L.; Zhang, S.; Ma, J.; Dong, W.; Zeng, Y.; Yuan, J.; Liu, C.; Luo, S. "Dark Deposition" of Ag Nanoparticles on TiO_2: Improvement of Electron Storage Capacity To Boost "Memory Catalysis" Activity. *ACS Appl. Mater. Interfaces* **2018**, *10*, 25350–25359. [CrossRef] [PubMed]

34. Prakash, J. Mechanistic Insights into Graphene Oxide Driven Photocatalysis as Co-Catalyst and Sole Catalyst in Degradation of Organic Dye Pollutants. *Photochem* **2022**, *2*, 651–671. [CrossRef]

35. Verma, S.; Mal, D.S.; de Oliveira, P.R.; Janegitz, B.C.; Prakash, J.; Gupta, R.K. A facile synthesis of novel polyaniline/graphene nanocomposite thin films for enzyme-free electrochemical sensing of hydrogen peroxide. *Mol. Syst. Des. Eng.* **2022**, *7*, 158–170. [CrossRef]

36. Sharma, P.; Kherb, J.; Prakash, J.; Kaushal, R. A novel and facile green synthesis of SiO_2 nanoparticles for removal of toxic water pollutants. *Appl. Nanosci.* **2021**. [CrossRef]

37. Prakash, J.; Harris, R.A.; Swart, H.C. Embedded plasmonic nanostructures: Synthesis, fundamental aspects and their surface enhanced Raman scattering applications. *Int. Rev. Phys. Chem.* **2016**, *35*, 353–398. [CrossRef]

38. Qi, K.; Cheng, B.; Yu, J.; Ho, W. A review on TiO_2-based Z-scheme photocatalysts. *Chin. J. Catal.* **2017**, *38*, 1936–1955. [CrossRef]

39. Yu, J.; Wang, W.; Cheng, B.; Su, B.-L. Enhancement of Photocatalytic Activity of Mesoporous TiO_2 Powders by Hydrothermal Surface Fluorination Treatment. *J. Phys. Chem. C* **2009**, *113*, 6743–6750. [CrossRef]

40. Yu, J.C.; Yu, J.; Ho, W.; Jiang, Z.; Zhang, L. Effects of F- Doping on the Photocatalytic Activity and Microstructures of Nanocrystalline TiO_2 Powders. *Chem. Mater.* **2002**, *14*, 3808–3816. [CrossRef]

41. Li, J.; Ren, D.; Wu, Z.; Huang, C.; Yang, H.; Chen, Y.; Yu, H. Visible-light-mediated antifungal bamboo based on Fe-doped TiO_2 thin films. *RSC Adv.* **2017**, *7*, 55131–55140. [CrossRef]

42. Kumar, P.; Mathpal, M.C.; Prakash, J.; Jagannath, G.; Roos, W.D.; Swart, H.C. Plasmonic and nonlinear optical behavior of nanostructures in glass matrix for photonics application. *Mater. Res. Bull.* **2020**, *125*, 110799. [CrossRef]

43. Prakash, J.; Tripathi, A.; Gautam, S.; Chae, K.H.; Song, J.; Rigato, V.; Tripathi, J.; Asokan, K. Phenomenological understanding of dewetting and embedding of noble metal nanoparticles in thin films induced by ion irradiation. *Mater. Chem. Phys.* **2014**, *147*, 920–924. [CrossRef]

44. Kumar, P.; Mathpal, M.C.; Jagannath, G.; Prakash, J.; Maze, J.-R.; Roos, W.D.; Swart, H.C. Optical limiting applications of resonating plasmonic Au nanoparticles in a dielectric glass medium. *Nanotechnology* **2021**, *32*, 345709. [CrossRef]

45. Li, J.; Ma, R.; Wu, Z.; He, S.; Chen, Y.; Bai, R.; Wang, J. Visible-Light-Driven Ag-Modified TiO_2 Thin Films Anchored on Bamboo Material with Antifungal Memory Activity against *Aspergillus niger*. *J. Fungi* **2021**, *7*, 592. [CrossRef]

46. Ma, R.; Li, J.; Han, S.; Wu, Z.; Bao, Y.; He, S.; Chen, Y. Solar-driven $WO_3 \cdot H_2O/TiO_2$ heterojunction films immobilized onto bamboo biotemplate: Relationship between physical color, crystal structure, crystal morphology, and energy storage ability. *Surf. Interfaces* **2022**, *31*, 102028. [CrossRef]

47. Tatsuma, T.; Takeda, S.; Saitoh, S.; Ohko, Y.; Fujishima, A. Bactericidal effect of an energy storage TiO_2–WO_3 photocatalyst in dark. *Electrochem. Commun.* **2003**, *5*, 793–796. [CrossRef]

48. Singh, J.P.; Chen, C.L.; Dong, C.L.; Prakash, J.; Kabiraj, D.; Kanjilal, D.; Pong, W.F.; Asokan, K. Role of surface and subsurface defects in MgO thin film: XANES and magnetic investigations. *Superlattices Microstruct.* **2015**, *77*, 313–324. [CrossRef]

49. Pathak, T.K.; Kumar, V.; Prakash, J.; Purohit, L.P.; Swart, H.C.; Kroon, R.E. Fabrication and characterization of nitrogen doped p-ZnO on n-Si heterojunctions. *Sens. Actuators A. Phys.* **2016**, *247*, 475–481. [CrossRef]

50. Patel, S.P.; Chawla, A.K.; Chandra, R.; Prakash, J.; Kulriya, P.K.; Pivin, J.C.; Kanjilal, D.; Kumar, L. Structural phase transformation in ZnS nanocrystalline thin films by swift heavy ion irradiation. *Solid State Commun.* **2010**, *150*, 1158–1161. [CrossRef]

51. Chen, Z.; Zhang, G.; Prakash, J.; Zheng, Y.; Sun, S. Rational Design of Novel Catalysts with Atomic Layer Deposition for the Reduction of Carbon Dioxide. *Adv. Energy Mater.* **2019**, *9*, 1900889. [CrossRef]

52. Prakash, J.; Tripathi, A.; Khan, S.A.; Pivin, J.C.; Singh, F.; Tripathi, J.; Kumar, S.; Avasthi, D.K. Ion beam induced interface mixing of Ni on PTFE bilayer system studied by quadrupole mass analysis and electron spectroscopy for chemical analysis. *Vacuum* **2010**, *84*, 1275–1279. [CrossRef]

53. Prakash, J.; Swart, H.C.; Zhang, G.; Sun, S. Emerging applications of atomic layer deposition for the rational design of novel nanostructures for surface-enhanced Raman scattering. *J. Mater. Chem. C* **2019**, *7*, 1447–1471. [CrossRef]

54. Prakash, J. Fundamentals and applications of recyclable SERS substrates. *Int. Rev. Phys. Chem.* **2019**, *38*, 201–242. [CrossRef]

55. Singh, N.; Prakash, J.; Misra, M.; Sharma, A.; Gupta, R.K. Dual Functional Ta-Doped Electrospun TiO_2 Nanofibers with Enhanced Photocatalysis and SERS Detection for Organic Compounds. *ACS Appl. Mater. Interfaces* **2017**, *9*, 28495–28507. [CrossRef]

56. Krumdieck, S.P.; Boichot, R.; Gorthy, R.; Land, J.G.; Lay, S.; Gardecka, A.J.; Polson, M.I.J.; Wasa, A.; Aitken, J.E.; Heinemann, J.A.; et al. Nanostructured TiO_2 anatase-rutile-carbon solid coating with visible light antimicrobial activity. *Sci. Rep.* **2019**, *9*, 1883. [CrossRef]

57. Wanag, A.; Rokicka, P.; Kusiak-Nejman, E.; Kapica-Kozar, J.; Wrobel, R.J.; Markowska-Szczupak, A.; Morawski, A.W. Antibacterial properties of TiO_2 modified with reduced graphene oxide. *Ecotoxicol. Environ. Saf.* **2018**, *147*, 788–793. [CrossRef]

58. Zhou, X.; Zhou, M.; Ye, S.; Xu, Y.; Zhou, S.; Cai, Q.; Xie, G.; Huang, L.; Zheng, L.; Li, Y. Antibacterial activity and mechanism of the graphene oxide (rGO)- modified TiO_2 catalyst against Enterobacter hormaechei. *Int. Biodeterior. Biodegrad.* **2021**, *162*, 105260. [CrossRef]

59. Rokicka-Konieczna, P.; Wanag, A.; Sienkiewicz, A.; Kusiak-Nejman, E.; Morawski, A.W. Antibacterial effect of TiO_2 nanoparticles modified with APTES. *Catal. Commun.* **2020**, *134*, 105862. [CrossRef]

60. Dhanasekar, M.; Jenefer, V.; Nambiar, R.B.; Babu, S.G.; Selvam, S.P.; Neppolian, B.; Bhat, S.V. Ambient light antimicrobial activity of reduced graphene oxide supported metal doped TiO$_2$ nanoparticles and their PVA based polymer nanocomposite films. *Mater. Res. Bull.* **2018**, *97*, 238–243. [CrossRef]

61. Bonnefond, A.; González, E.; Asua, J.M.; Leiza, J.R.; Kiwi, J.; Pulgarin, C.; Rtimi, S. New evidence for hybrid acrylic/TiO$_2$ films inducing bacterial inactivation under low intensity simulated sunlight. *Colloids Surf. B. Biointerfaces* **2015**, *135*, 1–7. [CrossRef]

62. Lin, Y.-P.; Ksari, Y.; Prakash, J.; Giovanelli, L.; Valmalette, J.-C.; Themlin, J.-M. Nitrogen-doping processes of graphene by a versatile plasma-based method. *Carbon* **2014**, *73*, 216–224. [CrossRef]

63. Komba, N.; Zhang, G.; Wei, Q.; Yang, X.; Prakash, J.; Chenitz, R.; Rosei, F.; Sun, S. Iron (II) phthalocyanine/N-doped graphene: A highly efficient non-precious metal catalyst for oxygen reduction. *Int. J. Hydrog. Energy* **2019**, *44*, 18103–18114. [CrossRef]

64. Prakash, J.; Pivin, J.C.; Swart, H.C. Noble metal nanoparticles embedding into polymeric materials: From fundamentals to applications. *Adv. Colloid Interface Sci.* **2015**, *226*, 187–202. [CrossRef] [PubMed]

65. Hernández-Gordillo, A.; Arriaga, S. Mesoporous TiO$_2$ Monoliths Impregnated with CdS and CuO Nanoparticles for Airborne Bacteria Inactivation Under Visible Light. *Catal. Lett.* **2022**, *152*, 629–640. [CrossRef]

66. Islam, M.A.; Ikeguchi, A.; Naide, T. Effectiveness of an air cleaner device in reducing aerosol numbers and airborne bacteria from an enclosed type dairy barn. *Environ. Sci. Pollut. Res.* **2022**, *29*, 53022–53035. [CrossRef]

67. Lee, M.; Koziel, J.A.; Macedo, N.R.; Li, P.; Chen, B.; Jenks, W.S.; Zimmerman, J.; Paris, R.V. Mitigation of Particulate Matter and Airborne Pathogens in Swine Barn Emissions with Filtration and UV-A Photocatalysis. *Catalysts* **2021**, *11*, 1302. [CrossRef]

68. Valdez-Castillo, M.; Saucedo-Lucero, J.O.; Arriaga, S. Photocatalytic inactivation of airborne microorganisms in continuous flow using perlite-supported ZnO and TiO$_2$. *Chem. Eng. J.* **2019**, *374*, 914–923. [CrossRef]

69. Urbonavicius, M.; Varnagiris, S.; Sakalauskaite, S.; Demikyte, E.; Tuckute, S.; Lelis, M. Application of Floating TiO$_2$ Photocatalyst for Methylene Blue Decomposition and *Salmonella typhimurium* Inactivation. *Catalysts* **2021**, *11*, 794. [CrossRef]

70. Varnagiris, S.; Urbonavicius, M.; Sakalauskaite, S.; Daugelavicius, R.; Pranevicius, L.; Lelis, M.; Milcius, D. Floating TiO$_2$ photocatalyst for efficient inactivation of *E. coli* and decomposition of methylene blue solution. *Sci. Total Environ.* **2020**, *720*, 137600. [CrossRef]

71. Sboui, M.; Lachheb, H.; Bouattour, S.; Gruttadauria, M.; La Parola, V.; Liotta, L.F.; Boufi, S. TiO$_2$/Ag$_2$O immobilized on cellulose paper: A new floating system for enhanced photocatalytic and antibacterial activities. *Environ. Res.* **2021**, *198*, 111257. [CrossRef]

72. Mathur, G. COVID Killing Air Purifier Based on UV & Titanium Dioxide Based Photocatalysis System. *SAE Int. J. Adv. Curr. Pract. Mobil.* **2021**, *4*, 143–150.

73. Nakano, R.; Yamaguchi, A.; Sunada, K.; Nagai, T.; Nakano, A.; Suzuki, Y.; Yano, H.; Ishiguro, H.; Miyauchi, M. Inactivation of various variant types of SARS-CoV-2 by indoor-light-sensitive TiO2-based photocatalyst. *Sci. Rep.* **2022**, *12*, 5804. [CrossRef]

74. Uppal, T.; Reganti, S.; Martin, E.; Verma, S.C. Surface Inactivation of Human Coronavirus by MACOMA^{TM} UVA-TiO$_2$ Coupled Photocatalytic Disinfection System. *Catalysts* **2022**, *12*, 690. [CrossRef]

75. Zan, L.; Fa, W.; Peng, T.; Gong, Z.-K. Photocatalysis effect of nanometer TiO$_2$ and TiO$_2$-coated ceramic plate on Hepatitis B virus. *J. Photochem. Photobiol. B Biol.* **2007**, *86*, 165–169. [CrossRef]

76. Bhardwaj, S.K.; Singh, H.; Deep, A.; Khatri, M.; Bhaumik, J.; Kim, K.-H.; Bhardwaj, N. UVC-based photoinactivation as an efficient tool to control the transmission of coronaviruses. *Sci. Total Environ.* **2021**, *792*, 148548. [CrossRef]

77. Micochova, P.; Chadha, A.; Hesseloj, T.; Fraternali, F.; Ramsden, J.; Gupta, R. Rapid inactivation of SARS-CoV-2 by titanium dioxide surface coating. *Wellcome Open Res.* **2021**, *6*, 56. [CrossRef]

78. Kupferschmidt, K.; Wadman, M. Delta variant triggers new phase in the pandemic. *Science* **2021**, *372*, 1375–1376. [CrossRef]

79. Sharma, D.K.; Shukla, S.; Sharma, K.K.; Kumar, V. A review on ZnO: Fundamental properties and applications. *Mater. Today Proc.* **2020**, *49*, 3028–3035. [CrossRef]

80. Yamada, H.; Suzuki, K.; Koizumi, S. Gene expression profile in human cells exposed to zinc. *J. Toxicol. Sci.* **2007**, *32*, 193–196. [CrossRef]

81. Umar, A.; Rahman, M.; Vaseem, M.; Hahn, Y.-B. Ultra-sensitive cholesterol biosensor based on low-temperature grown ZnO nanoparticles. *Electrochem. Commun.* **2009**, *11*, 118–121. [CrossRef]

82. Sharmila, G.; Muthukumaran, C.; Sandiya, K.; Santhiya, S.; Pradeep, R.S.; Kumar, N.M.; Suriyanarayanan, N.; Thirumarimurugan, M. Biosynthesis, characterization, and antibacterial activity of zinc oxide nanoparticles derived from Bauhinia tomentosa leaf extract. *J. Nanostruct. Chem.* **2018**, *8*, 293–299. [CrossRef]

83. Sportelli, M.C.; Izzi, M.; Loconsole, D.; Sallustio, A.; Picca, R.A.; Felici, R.; Chironna, M.; Cioffi, N. On the Efficacy of ZnO Nanostructures against SARS-CoV-2. *Int. J. Mol. Sci.* **2022**, *23*, 3040. [CrossRef]

84. Raj, N.B.; PavithraGowda, N.; Pooja, O.; Purushotham, B.; Kumar, M.A.; Sukrutha, S.; Ravikumar, C.; Nagaswarupa, H.; Murthy, H.A.; Boppana, S.B. Harnessing ZnO nanoparticles for antimicrobial and photocatalytic activities. *J. Photochem. Photobiol.* **2021**, *6*, 100021. [CrossRef]

85. Milionis, A.; Tripathy, A.; Donati, M.; Sharma, C.S.; Pan, F.; Maniura-Weber, K.; Ren, Q.; Poulikakos, D. Water-based scalable methods for self-cleaning antibacterial ZnO-nanostructured surfaces. *Ind. Eng. Chem. Res.* **2020**, *59*, 14323–14333. [CrossRef]

86. Prakash, J.; Kumar, V.; Erasmus, L.J.B.; Duvenhage, M.M.; Sathiyan, G.; Bellucci, S.; Sun, S.; Swart, H.C. Phosphor Polymer Nanocomposite: ZnO:Tb3+ Embedded Polystyrene Nanocomposite Thin Films for Solid-State Lighting Applications. *ACS Appl. Nano Mater.* **2018**, *1*, 977–988. [CrossRef]

87. Kumar, R.S.; Dananjaya, S.H.S.; De Zoysa, M.; Yang, M. Enhanced antifungal activity of Ni-doped ZnO nanostructures under dark conditions. *RSC Adv.* **2016**, *6*, 108468–108476. [CrossRef]

88. Iqbal, G.; Faisal, S.; Khan, S.; Shams, D.F.; Nadhman, A. Photo-inactivation and efflux pump inhibition of methicillin resistant Staphylococcus aureus using thiolated cobalt doped ZnO nanoparticles. *J. Photochem. Photobiol. B Biol.* **2019**, *192*, 141–146. [CrossRef]

89. Vijayalakshmi, K.; Sivaraj, D. Enhanced antibacterial activity of Cr doped ZnO nanorods synthesized using microwave processing. *RSC Adv.* **2015**, *5*, 68461–68469. [CrossRef]

90. Naskar, A.; Lee, S.; Kim, K.-S. Antibacterial potential of Ni-doped zinc oxide nanostructure: Comparatively more effective against Gram-negative bacteria including multi-drug resistant strains. *RSC Adv.* **2020**, *10*, 1232–1242. [CrossRef]

91. Geetha, K.; Sivasangari, D.; Kim, H.-S.; Murugadoss, G.; Kathalingam, A. Electrospun nanofibrous ZnO/PVA/PVP composite films for efficient antimicrobial face masks. *Ceram. Int.* **2022**, *48*, 29197–29204. [CrossRef]

92. Attia, G.H.; Moemen, Y.S.; Youns, M.; Ibrahim, A.M.; Abdou, R.; El Raey, M.A. Antiviral zinc oxide nanoparticles mediated by hesperidin and in silico comparison study between antiviral phenolics as anti-SARS-CoV-2. *Colloids Surf. B Biointerfaces* **2021**, *203*, 111724. [CrossRef] [PubMed]

93. Hamdi, M.; Abdel-Bar, H.M.; Elmowafy, E.; El-Khouly, A.; Mansour, M.; Awad, G.A. Investigating the internalization and COVID-19 antiviral computational analysis of optimized nanoscale zinc oxide. *ACS Omega* **2021**, *6*, 6848–6860. [CrossRef] [PubMed]

94. El-Megharbel, S.M.; Alsawat, M.; Al-Salmi, F.A.; Hamza, R.Z. Utilizing of (zinc oxide nano-spray) for disinfection against "SARS-CoV-2" and testing its biological effectiveness on some biochemical parameters during (COVID-19 pandemic)—"ZnO nanoparticles have antiviral activity against (SARS-CoV-2)". *Coatings* **2021**, *11*, 388. [CrossRef]

95. Ishida, T. Anti-viral vaccine activity of Zinc (II) for viral prevention, entry, replication, and spreading during pathogenesis process. *Curr. Trends. Biomed. Eng. Biosci.* **2019**, *19*, MS.ID.556012. [CrossRef]

96. Antoine, T.E.; Mishra, Y.K.; Trigilio, J.; Tiwari, V.; Adelung, R.; Shukla, D. Prophylactic, therapeutic and neutralizing effects of zinc oxide tetrapod structures against herpes simplex virus type-2 infection. *Antivir. Res.* **2012**, *96*, 363–375. [CrossRef]

97. Siddiqi, K.S.; Rahman, A.U.; Tajuddin, H.A. Properties of Zinc Oxide Nanoparticles and Their Activity Against Microbes. *Nanoscale Res. Lett.* **2018**, *13*, 141. [CrossRef]

98. Prasad, A.S. Zinc in human health: Effect of zinc on immune cells. *Mol. Med.* **2008**, *14*, 353–357. [CrossRef]

99. Te Velthuis, A.J.; van den Worm, S.H.; Sims, A.C.; Baric, R.S.; Snijder, E.J.; van Hemert, M.J. Zn^{2+} inhibits coronavirus and arterivirus RNA polymerase activity in vitro and zinc ionophores block the replication of these viruses in cell culture. *PLoS Pathog.* **2010**, *6*, e1001176. [CrossRef]

100. Kalsi, T.; Mitra, H.; Roy, T.K.; Godara, S.K.; Kumar, P. Comprehensive Analysis of Band Gap and Nanotwinning in Cd1–xMgxS QDs. *Cryst. Growth Des.* **2020**, *20*, 6699–6706. [CrossRef]

101. Jiang, J.; Pi, J.; Cai, J. The advancing of zinc oxide nanoparticles for biomedical applications. *Bioinorg. Chem. Appl.* **2018**, *2018*, 1062562. [CrossRef]

102. Momeni, M.; Mirhosseini, M.; Nazari, Z.; Kazempour, A.; Hakimiyan, M. Antibacterial and photocatalytic activity of CuO nanostructure films with different morphology. *J. Mater. Sci. Mater. Electron.* **2016**, *27*, 8131–8137. [CrossRef]

103. Pugazhendhi, A.; Kumar, S.S.; Manikandan, M.; Saravanan, M. Photocatalytic properties and antimicrobial efficacy of Fe doped, CuO nanoparticles against the pathogenic bacteria and fungi. *Microb. Pathog.* **2018**, *122*, 84–89. [CrossRef]

104. Giti, R.; Zomorodian, K.; Firouzmandi, M.; Zareshahrabadi, Z.; Rahmannasab, S. Antimicrobial activity of thermocycled polymethyl methacrylate resin reinforced with titanium dioxide and copper oxide nanoparticles. *Int. J. Dent.* **2021**, *2021*, 6690806. [CrossRef]

105. Wang, L.; Hu, C.; Shao, L. The antimicrobial activity of nanoparticles: Present situation and prospects for the future. *Int. J. Nanomed.* **2017**, *12*, 1227. [CrossRef]

106. Soni, V.; Xia, C.; Cheng, C.K.; Nguyen, V.-H.; Nguyen, D.L.T.; Bajpai, A.; Kim, S.Y.; Van Le, Q.; Khan, A.A.P.; Singh, P. Advances and recent trends in cobalt-based cocatalysts for solar-to-fuel conversion. *Appl. Mater. Today* **2021**, *24*, 101074. [CrossRef]

107. Bandala, E.R.; Kruger, B.R.; Cesarino, I.; Leao, A.L.; Wijesiri, B.; Goonetilleke, A. Impacts of COVID-19 pandemic on the wastewater pathway into surface water: A review. *Sci. Total Environ.* **2021**, *774*, 145586. [CrossRef]

108. Ghotekar, S.; Pansambal, S.; Bilal, M.; Pingale, S.S.; Oza, R. Environmentally friendly synthesis of Cr2O3 nanoparticles: Characterization, applications and future perspective—A review. *Case Stud. Chem. Environ. Eng.* **2021**, *3*, 100089. [CrossRef]

109. Tavakoli, A.; Hashemzadeh, M.S. Inhibition of herpes simplex virus type 1 by copper oxide nanoparticles. *J. Virol. Methods* **2020**, *275*, 113688. [CrossRef]

110. Dulta, K.; Ağçeli, G.K.; Chauhan, P.; Jasrotia, R.; Ighalo, J.O. Multifunctional CuO nanoparticles with enhanced photocatalytic dye degradation and antibacterial activity. *Sustain. Environ. Res.* **2022**, *32*, 1–15. [CrossRef]

111. Akhavan, O.; Azimirad, R.; Safa, S.; Hasani, E. CuO/Cu(OH)2 hierarchical nanostructures as bactericidal photocatalysts. *J. Mater. Chem.* **2011**, *21*, 9634–9640. [CrossRef]

112. Akhavan, O.; Ghaderi, E. Cu and CuO nanoparticles immobilized by silica thin films as antibacterial materials and photocatalysts. *Surf. Coat. Technol.* **2010**, *205*, 219–223. [CrossRef]

113. Gurianov, Y.; Nakonechny, F.; Albo, Y.; Nisnevitch, M. Antibacterial composites of cuprous oxide nanoparticles and polyethylene. *Int. J. Mol. Sci.* **2019**, *20*, 439. [CrossRef]

114. Domagała, E. Stability evaluation of Cu₂O/MWCNTs filters for virus removal from water. *Water Res.* **2020**, *179*, 115879. [CrossRef]

115. Mazurkow, J.M.; Yüzbasi, N.S.; Domagala, K.W.; Pfeiffer, S.; Kata, D.; Graule, T. Nano-sized copper (oxide) on alumina granules for water filtration: Effect of copper oxidation state on virus removal performance. *Environ. Sci. Technol.* **2019**, *54*, 1214–1222. [CrossRef] [PubMed]

116. Amiri, M.; Etemadifar, Z.; Daneshkazemi, A.; Nateghi, M. Antimicrobial effect of copper oxide nanoparticles on some oral bacteria and candida species. *J. Dent. Biomater.* **2017**, *4*, 347. [PubMed]

117. Hang, X.; Peng, H.; Song, H.; Qi, Z.; Miao, X.; Xu, W. Antiviral activity of cuprous oxide nanoparticles against Hepatitis C Virus in vitro. *J. Virol. Methods* **2015**, *222*, 150–157. [CrossRef] [PubMed]

118. Borkow, G.; Zhou, S.S.; Page, T.; Gabbay, J. A novel anti-influenza copper oxide containing respiratory face mask. *PLoS ONE* **2010**, *5*, e11295. [CrossRef] [PubMed]

119. Leung, N.H.; Chu, D.K.; Shiu, E.Y.; Chan, K.H.; McDevitt, J.J.; Hau, B.J.; Cowling, B.J. Respiratory virus shedding in exhaled breath and efficacy of face masks. *Nat. Med.* **2020**, *26*, 676–680. [CrossRef]

120. Hosseini, M.; Chin, A.W.; Behzadinasab, S.; Poon, L.L.; Ducker, W.A. Cupric oxide coating that rapidly reduces infection by SARS-CoV-2 via solids. *ACS Appl. Mater. Interfaces* **2021**, *13*, 5919–5928. [CrossRef]

121. Merkl, P.; Long, S.; McInerney, G.M.; Sotiriou, G.A. Antiviral activity of silver, copper oxide and zinc oxide nanoparticle coatings against SARS-CoV-2. *Nanomaterials* **2021**, *11*, 1312. [CrossRef]

122. Delumeau, L.V.; Asgarimoghaddam, H.; Alkie, T.; Jones, A.J.B.; Lum, S.; Mistry, K.; Musselman, K.P. Effectiveness of antiviral metal and metal oxide thin-film coatings against human coronavirus 229E. *APL Mater.* **2021**, *9*, 111114. [CrossRef]

123. Farah, J.; Ibadurrohman, M.; Slamet. Synthesis of CuO-TiO₂ nano-composite for Escherichia coli disinfection and toluene degradation. *AIP Conf. Proc.* **2020**, *2237*, 020050.

124. Kanako, Y.; Yui, S.; Momo, I.; Takakiyo, T.; Toshikazu, S.; Jin-ichi, S. Photocatalytic Antibacterial Activity of TiO₂, TiO₂+CuO, and WO₃ +CuO -Evaluation of Codoping Effect. *Technol. Innov. Pharm. Res.* **2021**, *1*, 130–139.

125. Uema, M.; Yonemitsu, K.; Momose, Y.; Ishii, Y.; Tateda, K.; Inoue, T.; Asakura, H. Effect of the Photocatalyst under Visible Light Irradiation in SARS-CoV-2 Stability on an Abiotic Surface. *Biocontrol Sci.* **2021**, *26*, 119–125. [CrossRef]

126. Lin, H.; Li, T.; Janani, B.J.; Fakhri, A. Fabrication of Cu₂MoS₄ decorated WO₃ nano heterojunction embedded on chitosan: Robust photocatalytic efficiency, antibacterial performance, and bacteria detection by peroxidase activity. *J. Photochem. Photobiol. B Biol.* **2022**, *226*, 112354. [CrossRef]

127. Hojamberdiev, M.; Czech, B.; Wasilewska, A.; Boguszewska-Czubara, A.; Yubuta, K.; Wagata, H.; Daminova, S.S.; Kadirova, Z.C.; Vargas, R. Detoxifying SARS-CoV-2 antiviral drugs from model and real wastewaters by industrial waste-derived multiphase photocatalysts. *J. Hazard. Mater.* **2022**, *429*, 128300. [CrossRef]

128. Czech, B.; Krzyszczak, A.; Boguszewska-Czubara, A.; Opielak, G.; Jośko, I.; Hojamberdiev, M. Revealing the toxicity of lopinavir- and ritonavir-containing water and wastewater treated by photo-induced processes to Danio rerio and Allivibrio fischeri. *Sci. Total Environ.* **2022**, *824*, 153967. [CrossRef]

129. Teymoorian, T.; Teymourian, T.; Kowsari, E.; Ramakrishna, S. Direct and indirect effects of SARS-CoV-2 on wastewater treatment. *J. Water Process Eng.* **2021**, *42*, 102193. [CrossRef]

130. Yang, J.Z.Y.; Gou, X.; Pu, K.; Chen, Z.; Guo, Q.; Ji, R.; Wang, H.; Wang, Y.; Zhou, Y. Prevalence of comorbidities and its effects in patients infected with SARS-CoV-2: A systematic review and meta-analysis. *Int. J. Infect. Dis.* **2020**, *94*, 91–95. [CrossRef]

131. Huang, F.L.Y.; Leung, E.L.; Liu, X.; Liu, K.; Wang, Q.; Lan, Y.; Li, X.; Yu, H.; Cui, L.; Luo, H.; et al. A review of therapeutic agents and Chinese herbal medicines against SARS-COV-2 (COVID-19). *Pharm. Res.* **2020**, *158*, 104929. [CrossRef]

132. Elgohary, E.A.; Mohamed, Y.M.A.; El Nazer, H.A.; Baaloudj, O.; Alyami, M.S.S.; El Jery, A.; Assadi, A.A.; Amrane, A. A Review of the Use of Semiconductors as Catalysts in the Photocatalytic Inactivation of Microorganisms. *Catalysts* **2021**, *11*, 1498. [CrossRef]

133. Sanvicens, N.; Marco, M.P. Multifunctional nanoparticles–properties and prospects for their use in human medicine. *Trends Biotechnol.* **2008**, *26*, 425–433. [CrossRef]

134. Seabra, A.B.; Durán, N. Nanotoxicology of metal oxide nanoparticles. *Metals* **2015**, *5*, 934–975. [CrossRef]